A THESIS SUBMITTED TO
THE GRADUATE SCHOOL OF NATURAL AND APPLIED SCIENCES
OF ÇANKIRI KARATEKİN UNIVERSITY

SPACE VECTOR PULSE WIDTH MODULATION BASED SPEED CONTROL OF INDUCTION MOTOR WITH THREE LEVEL INVERTER USING VOLTAGE/FREQUENCY CONTROLLER

IN PARTIAL FULFILLMENT OF THE REQUIREMENTS
FOR
THE DEGREE OF MASTER OF SCIENCE
IN
ELECTRICAL AND ELECTRONICS ENGINEERING

BY

AHMED HARB NAJD NAJD

ÇANKIRI

2021

SPACE VECTOR PULSE WIDTH MODULATION BASED SPEED CONTROL OF INDUCTION MOTOR WITH THREE LEVEL INVERTER USING VOLTAGE/FREQUENCY CONTROLLER

By Ahmed Harb Najd NAJD

August 2021

We certify that we have read this thesis and that in our opinion it is fully adequate, in scope and in quality, as a thesis for the degree of Master of Science

Advisor **:** Assoc. Prof. Dr. Fatih KORKMAZ

Examining Committee Members:

Chairman **:** Assoc. Prof. Dr. Hayati MAMUR
Electrical and Electronics Engineering
Manisa Celal Bayar University

Member **:** Assoc. Prof. Dr. Fatih KORKMAZ
Electrical and Electronics Engineering
Çankırı Karatekin University

Member **:** Asst. Prof. Dr. İsmail TOPALOGLU
Electrical and Electronics Engineering
Çankırı Karatekin University

Approved for the Graduate School of Natural and Applied Sciences

Prof. Dr. İbrahim ÇİFTÇİ
Director of Graduate School

I hereby declare that all information in this document has been obtained and presented in accordance with academic rules and ethical conduct. I also declare that, as required by these rules and conduct, I have fully cited and referenced all material and results that are not original to this work.

Ahmed Harb Najd NAJD

ABSTRACT

SPACE VECTOR PULSE WIDTH MODULATION BASED SPEED CONTROL OF INDUCTION MOTOR WITH THREE LEVEL INVERTER USING VOLTAGE/FREQUENCY CONTROLLER

Ahmed Harb Najd NAJD
Master of Science in Electrical and Electronics Engineering
Advisor: Assoc. Prof. Dr. Fatih KORKMAZ
August 2021

In general, speed control is an essential technology in flexible fast driving systems. To achieve that it requests variable frequency and voltage supply. Even though there are numbers of the pulse width modulation (PWM) scheme is utilized to get the variable frequency and supply voltage from an inverter. It is less used than the space vector pulse width modulation (SVPWM). The SVPWM method with supply voltage/frequency (V/f) control of induction motor (IM) is an alternating current (AC) motor that converts electrical energy into kinetic energy and drive is vastly utilized in the high-performance drive system. It is due to its characteristics such as high efficiency and good power factor. In this study, the voltage source inverter type SVPWM with three-level inverter using (V/f) control model design and implementation has been done through Matlab/Simulink software for the speed control of an IM. The proposed SVPWM for a three-level voltage-fed inverter, extended to the over modulation range. The over modulation strategy easily blends with the under modulation so that the inverter can operate smoothly from low speed to the extended speed range. The simulation results offer that the proposed three-level inverter reduces undulations in speed and torque.

2021, 73 pages

Keywords: Induction motor, SVPWM, V/f control

ÖZET

İNDÜKSİYON MOTORUN ÜÇ SEVİYELİ İNVERTER KULLANILAN V/F DENETLİYİCİ İLE UZAY VEKTÖR DARBE GENİŞLİK MODÜLASYONU BAZLI HIZ KONTROLÜ

Ahmed Harb Najd NAJD
Elektrik-Elektronik Mühendisliği, Yüksek Lisans
Tez Danışmanı: Doç. Dr. Fatih KORKMAZ
Ağustos 2021

Genel olarak, hız kontrolü, esnek hızlı sürüş sistemlerinde önemli bir teknolojidir. Bunu başarmak için değişken frekans ve voltaj beslemesi talep eder. Darbe genişlik modülasyonu (PWM) şemasının sayısı olmasına rağmen, bir inverterden değişken frekans ve besleme voltajı elde etmek için kullanılır. Uzay vektör darbe genişlik modülasyonundan (SVPWM) daha az kullanılır. Asenkron motor sürücüsünün besleme voltaj/frekans (V/f) kontrolüne sahip SVPWM yöntemi, yüksek performanslı sürücü sisteminde büyük ölçüde kullanılmaktadır. Yüksek verimlilik ve iyi güç faktörü gibi özelliklerinden kaynaklanmaktadır. Bu çalışmada, asenkron motorun hız kontrolü için matlab / simülasyon yazılımı kullanılarak V/f kontrol modeli kullanılarak üç seviyeli invertörlü gerilim kaynaklı inverter tipi SVPWM tasarımı ve uygulaması yapılmıştır. Üç seviyeli voltaj beslemeli bir invertör için önerilen SVPWM, aşırı modülasyon aralığına genişletildi. Aşırı modülasyon stratejisi, düşük modülasyonla kolayca karışır, böylece inverter, düşük hızdan genişletilmiş hız aralığına kadar sorunsuz bir şekilde çalışabilir. Simülasyon sonuçları, önerilen üç seviyeli invertörün hız ve torktaki dalgalanmaları azalttığını göstermektedir.

2021, 73 Sayfa

Anahtar Kelimeler: İndüksiyon motor, SVPWM, V/f kontrolü

PREFACE AND ACKNOWLEDGEMENTS

I would like to thank my thesis advisor, Assoc. Prof. Dr. Fatih KORKMAZ, for his patience, guidance and understanding.

Ahmed Harb Najd NAJD
Çankırı-2021

CONTENTS

LIST OF SYMBOLS

f	Frequency
F_s	Magnetic Field Strength
F_r	The intensity of the Magnetic Field Rotor
I_n	Nominal Starting Current
I_1	Stator current
I_2	Rotor current
I_m	Magnetization Current
K_{w1}	Stator Winding Factor
K_{w2}	Rotor Winding Factor
N	Rotor Speed
N_s	Synchronous Speed
N_r	Rotor speed
n_s	Number Stator Turns
N_1	Equivalent circuit ideal transformer primary turns
N_2	Equivalent circuit ideal transformer secondary turns
$\emptyset_m$	Maximum Phase Flux
P	Number Pole
P	Power
P_1	Electrical Power
P_{cu1}	Missing power copper in Stator Coils
P_{core}	Power Losses the Motor
P_m	Generator Mechanical Power
P_g	Power of the Air Gap
P_f	Friction Losses Power
P_2	Mechanical Power Output
rpm	Rad per minute
R	Resistance
S	Slip in Induction Motor
T	Torque
Te	Electromagnetic Torque
T_f	Torque of the Mechanical Losses
V	Alpha Voltage
V_{beta}	Beta Voltage
V_{Ref}	Reference Voltage
ω_s	Angular Velocity of the Rotating Magnetic Field
ω	Angular Velocity of the Rotor
X	Leakage Reactance
X_1	Stator leakage reactance

X_2	Rotor circuit reactance
X_m	Magnetization reactance
$Z_{eq.}$	Equivalent Impedance

LIST OF ABBREVIATIONS

AC	Alternating Current
ANFIS	Adaptive Neuro-Fuzzy Inference System
cos Ø	Power Factor
DC	Direct Current
DSP	Digital Signal Processor
EMF	Electrical Motive Force
FPGA	Field Programmable Gate Arrays
FLC	Fuzzy Logic Controller
IM	Induction Motor
IGBT	Insulated-Gate Bipolar Transistor
NN	Neural Network
NNIS	Neural Network Inverse System
NPC	Neutral-Point Clamped
PI	Proportional Integral
PWM	Pulse Width Modulation
RTW	Real-Time Workshop
SVM	Space Vector Modulation
SPWM	Sinusoidal Pulse Width Modulation
SVPWM	Space Vector Pulse Width Modulation
THD	Total Harmonic Distortion
THPWM	Third-Harmonic Pulse Width Modulation
VFD	Variable-Frequency Drives
VSI	Voltage Source Inverter

LIST OF FIGURES

LIST OF TABLES

1. INTRODUCTION

Electric motors began to develop at the beginning of the nineteenth century, after discovering the electromagnet. The Danish physicist Hans Christians Oersted detected in 1820 that a cable in whose electric current passes creates around its magnetic domain. Moreover, when the current passes through a loop wire (formed in the shape of a ring), and stronger inside the ring the generated magnetic field, and the trend of the generated field is vertical to the level of the ring. In addition, American physicist Joseph Henry explained in the late 1820s that an electromagnet could be invented to be further strengthened by winding several turns of secluded wires about a segment of the ferric.

In addition, in 1821, the English physicist Michael Faraday hung a cupreous cable and sloping it into quicksilver's vessel. The quicksilver receptacle had a magnetic bar. When Faraday push through an electric current through the cable, it found that it began to orbit about the magnetism existing in quicksilver. In addition, Faraday found that the electric current created around the cable an orbicular magnetic domain. This experiment demonstrates how the electric motor works for students in schools, with Mercury being replaced by water with dissolved salt to be conductive because Mercury is a toxic substance. Its vapor is toxic as well as the hand-held experience of an electromagnetic rotor from 1827. (Budapest Museum of Applied Arts). Moreover, the historic engine is still running (Da Silva *et al*. 2013).

Furthermore, in 1827, the Hungarian physicist, Anusch Yelik, conducted an experiment using wire coils. He modified the experiment to consist of three components of a DC motor: a stator, a rotor, and an electrical exchanger. This device does not use a self-magnet but rather produces the two magnetic fields from the two electric currents passing through the stator windings and the rotor windings.

The first commercially successful DC motor appeared in 1873 by Zenob Theophil Gramm in Vienna (a Belgian electrical engineer). Theo Phil also presented a study that would improve the efficiency of primitive electric motors and generators.

In addition, Nikola Tesla invented (a Serbian engineer) the alternating current motor in 1888, and at the beginning of the twentieth century, many advanced electric motors were developed (Da Silva *et al.* 2013).

Moreover, in the first decade from the twentieth, many engineers and inventors experimented with linear electric motors. Instead of spinning, such motors produce an electromagnetic wave that can directly drive a vehicle. Likewise, this became more popular with the pioneering work of electrical engineer Eric Lei Thwaite in using the linear actuator from 1950 to 1960.

Furthermore, speed control methods of induction motors are an important topic because many manufacturing industries require a practical motor to carry out their works operations, so motor speed control is essential. To evaluate speed control method an efficient is necessary this method gives benefits like energy savings as well as cost-effectiveness etc. Due to flow full issues with induction engines with the voltage supplied to the engine should chance with the frequency. The induction engine leads V/f with inverters are largely utilized in manufacturing implementations not only for capacity keeping but also to get better quality and productivity. In connection with the study topic, the following literature has been studied.

Three-phase induction engine speed control is necessary due to the engine monitoring manufacture is a controlling section. To remnant competitive, new manufactures should be advanced that have many delineation sides such as lower cost, lower energy exhaustion, and get better power factor. To overcome these provocations, traditional procedures require to be modified by developed monitoring technicalities that enable to meet the above requirements with a high level of performance (Swamy and Kumar 2008). In the industrial sector, the squirrel cage engine is the ultimate widely utilized among all types of machines because it has proved such as rugged, frugal structure, low upkeep, capability to run in grubby or explosive stipulations, preferable and dependable performance, and is the change in a wide energy range. There are many modes of controlling the speed of a 3-phase engine, such as constant rotor resistance dominant, frequency control, and voltage control, but V/f velocity dominant is the ultimate commonly used mode in velocity dominant the ultimate common modes utilized in the adaptable velocity lead system. In the velocity domination technicality, the V/f ratio is to be preserved stable so that influx residues are stable (Hussain *et al*. 2012).

In addition, velocity domination technicalities are generally fundamental in an adaptable velocity drive system. This system requests change frequency and voltage supply which is positively gotten from a 3-phase voltage supply inverter (VSI). A numeral of pulse width modulation (PWM) planners are utilized to get a mutable frequency and voltage source from an inverter, such as sine (SPWM), third harmonic PWM (THPWM), and space vector pulse width modulation (SVPWM). There is a growing orientation to use space vector PWM (SVPWM) due to it is easier to implement digitally, makes better use of the DC bus, and the produced voltage is large like a sine wave (Majeed *et al*. 2020).

Further, the procedures a comparative study between the variations (PWM) technicalities inclusive, sinusoidal PWM (SPWM), multiple PWM (MPWM), and space vector pulse width modulation (SVPWM). These technicalities are defined, compared, and examined to produce gate pulses for a 3-phase (VSI). The modulation indicator is assorted for achieving the prorated analysis of these technicalities. PWM technicalities are recognized due to the minimum symmetrical purport got in the produce current and voltage, constant transition frequency, and rise peak employment of the DC bus. In addition, SVPWM is then utilized for achieving voltage/frequency (V/f) control of squirrel cage IM having variations in energy ratings (Divyam *et al*. 2020).

Besides, the speed control of IM by a 3-phase voltage supply inverter using the universal bridge and PWM method. A PID controller was used to surveillance the peak DC link voltage of the voltage supply inverter. The rendering analysis of the closed-loop and open-loop velocity surveillance of the regulation is carried out in Matlab/Simulink. The simulation outcome display that the velocity surveillance has perfect efficiency and the ability to successfully monitoring the IM with the best performance (Hartono *et al*. 2019).

Moreover, the velocity observer of an IFOC-based 3-phase IM drive is demanded to optimize the energy as it passes. Nevertheless, the monitoring system in IM is much complicated due to its nonlinearity and intricacy. In this study, it is numerical tuning speed controller is utilized as a proportional, integral, and derivative (PID) for monitor and subscribe the pass into velocity showing of IM through real-time control (RTC) on Matlab/Simulink and then combined with a 3-phase voltage supply inverter (VSI). Using RTC is a suitable, simple, and time-provident instrument on an IFOC-based IM drive to perform a speed controller in real-time without disturbing other complex languages programming. Further, founded on the empirical result by RTC, in this case, the PID speed controller has the best implementation and does not get surpass compared than the open-loop response (Ferdiansyah *et al*. 2018).

Additionally, presents other methods for monitoring a 3-phase IM based on the static V/f control technology. To suppress torque and stator flux variations while using SVM technology, PI controller, and DTC functions in both dynamic and steady-state. To generate phase angle references and static voltages to control an IM and shun the use of assortment converters, a static method V/f control is used. To perform this control method, the stator flux upgrade configuration is used as a complete supervisor. To get better the average approach, its feedback gain was designed under stability conditions, in particular in the low-velocity area of the observer to the left of the fictive axis in the level complex, and the real parts of these poles are separate from the engine velocity by placing the modern controlling magnates farther away from the old magnates (Attia 2018).

Multilevel inverters have been widely used in drive applications for several decades. Due to its incomparable advantages and because of its lower symmetrical content in the produces at top transition frequencies, the neutral point clamped (NPC) inverter has chosen space vector pulse width modulation (SV -PWM/SVM) for the analysis objective in this study (Sundararaju *et al*. 2017).

Moreover, an SVPWM-based three-stage NPC inverter with a unified transition series. The accorded delineation support in reducing the numeral of inverter transition frequencies in a peak transition frequency domain, contrasted to the traditional SV -PWM scheme, and provides the best moving response when supplied to any lead system, due to lower distortion factor and its different other proses (Divyam *et al*.2020).

Since the three-stage NPC inverter is largely suitable for medium voltage and rises energy implementations, they looked at the NPC transformer for the analysis. Moreover, the effects of load and velocity differences on stator velocity, torque, and current are presented in this study. The proposed sketch is compared with the performance of the applied (SPWM) design of the drive system. The offered monitoring design is established on the closest three vector sketch, without a research table. The proposed SVM design utilizes a small numeral of transition rotations and simplifies the periodic or duty cycles. Moreover, these transition rotations are diverse for every sector of the SVM graph (Sundararaju *et al*. 2017).

The (SVPWM) technique for multilevel cascaded H-bridge inverter (CHB inverter) and an equivalent DC voltage source with a resistive-inductive load. The CHB inverter generates a big numeral of voltage vectors and sprawling transition statuses, which is an issue of computational intricacy in the multilevel inverters. An unpretentious SVPWM delineation is offered to convergent the reference vector, and the computation of the well-posedness becomes much easy (Attia 2018). SVPWM offers many advantages: perfect utilization of the DC-link voltage, low current undulation, low symmetrical deformation, and lower transition reduction. A 3-phase multilevel CHB inverter has been built and simulation results are current to prove the national researches of the system model (Attia 2018).

In addition, a comparison between SPWM and SVPWM for three-phase two-phase inverters. It is increasingly used in numerous new manufacturing implementations that demand rise achievement by applying various pulse width modulation and control technologies. SVPWM and SPWM technology are most commonly used for 3-phase voltage source transformers (Annapurna and Tulasiramdas 2015).

A methodology for implementation accomplishment of a fuzzy-like PI observer for frequency tuning of an SVPWM inverter used for speed control for IM. In the control, the square ingredient of the stator current is predestined through the observer. Instead of a current observer, this study proposes to estimate the frequency of the stator voltage. The dynamic modeling of IM is represented by the dq-axis theory. From the simulation results, the proposed controller performs excellently in 3-phase IM speed control (Yaseen *et al.* 2018).

Furthermore, a comparison between two various PWM techniques utilize for a 3-phase (VSI) is discussed. The 3-phase (VSI) is the foundation topology utilized to source the network. In this study, designed an LC filter between the network and the inverter in order to settle the produced voltage. The filter grants sinusoidal 3-phase voltage at the output of the inverter with nearly zero/less symmetrical deformation. To get the requested output voltage on the line side of the inverter is utilized a suitable PWM technique. The PWM techniques used are based on SPWM and SVPWM (Umashankar *et al*. 2016).

The offers the equations of the mathematical version of a 3-phase induction engine limited inside the 3-phase stator reference structure. The skills of the proposed mathematical version are defined in detail. In special, the capability to version with their real frequency to the rotor currents. There is likewise an instance of modeling of the asynchronous machine on the ones a complicated version (Pustovetov 2017). It utilizes as a revolving electromechanical section splitter onboard a railroad electric-powered furl port. In this status, the device gets the delivered voltage from the secondary winding of a single-phase converter. Then it transformers it right into a three-section voltage to 3-phase customers along with induction engines loaded with the aid of using fanatics and air compressors. Simulation effects show the sufficiency of the advised mathematical version of the asynchronous electric-powered machines (Pustovetov 2017).

The precepts of implementing a control system using a PWM pocket inverter potentiometer and an induction motor vector control are reviewed. Comparisons are made between simplex control system with PWM control techniques and SPWM control with added third harmonic signal and modulated signal control. The maximum capacitance, actual values of the phase, and the output voltage of the line inverter were shown at the maximum amplitude of the control signals. Recommendations are given on the selection of a supply voltage induction electric motor with digital frequency control (Annapurna and Tulasiramdas 2015).

In addition, an induction motor (IM) was supplied to a voltage/frequency closed-loop control with skid arranging and its simulation outcomes utilized a based fuzzy logic controller. It is compared results fuzzy logic with a PID controller. IM is a model in expressions of d-q coils, with an asynchronous frame linked to the stator provocation frequency. The outcomes got in the simulation are motivating, with taken looking at the strong nonlinearity of the IM model. Fuzzy logic control for velocity observing of IM The simulation was advanced utilizing Fuzzy Matlab/Simulink. A fuzzy logic controller is incorporated into the regulation to conserve the velocity engine fixed while the load is different (Kamini *et al*. 2014).

Moreover, provides a recapitulation of advanced feeding methods and synchronous vector pulse PWM techniques for the voltage applied transformers, founded on criterion and non-criterion connotations to define pulse patterns. These PWM delineations are an applied theoretical in AC drive systems with the least ratio (frequency ratio) between the switch and transformer core frequencies, authorizing unwanted sub-symmetries in the current and voltage spectrums to be removed. The accent was performed on reviewing specified two-step delineations and diagrams for space-bound PWM, providing symmetries to the continuous voltage waveform of inverters in the perfect control area for any running conditions inclusive partial frequency ratios. Examples are provided for deploying synchronous PWM algorithms to switches and motor infrastructures (Oleschuk and Barrero 2014).

The speed control techniques are generally necessary for an adaptable speed drive system that requests variable voltage and supply at a frequency always got from a three-phase voltage supply inverter. A numeral of PWM schemes are utilized to get the change frequency and voltage source from the inverter, but space-to-space PWM has advantages such as easier digital perception, and the use of DC bus over other methods of pulse width modifications. The V/f speed control of a 3-phase IM by space vector modulation is demonstrated utilizing the Matlab/Simulink model (Raichurkar *et al*. 2016).

Further, the built and analyses of the VSI using three various techniques of PWM, such as third harmonic injection PWM (THIPWM), SPWM, and SVPWM. In alternating current, the fineness of the sine wave shape is more paramount than the goodness.

In require to achieve that, we are required to lessen the harmonic purport in the output. For that objective, several PWM technicalities are utilized. PWM technicalities are simulated for different loads and the outcomes are resolved with FFT analysis to note the total harmonic deformation (THD). The simulations are implemented in Matlab/Simulink programs (Nagasai and Jyothsna 2016).

Besides, the speed control of the IM using standard control technology. An IM due to its poor dynamic response compared to DC motors. With a VSI, it is likely to directly observe the stator flow e and electromagnetic torque connection through the optimal option of the inverter transition buses. Standard observe technology (V/f) is utilized due to simplicity of implementation of observing algorithm, better and accurate rejoinder with closed-loop slip reparations, and modeling of the IM drive using the V/f mode with the implementation of SVPWM is perfected in this study, it is preferable to comprehend the V/f mode and its intractable. During utilizing the three-level inverter, the undulations will be reduced in torque and velocity. The reference voltage vector is then recognized utilizing the voltage vector rate (Yadav 2016) .

1.1 The Aim of Thesis

The main aim of the have a look at is to broaden a model to put into effect V/f control of an induction motor. To do that, the PWM inverter drives the induction motor and PWM signal generation, and inverter topologies are studied and simulated.

Moreover, this research aims to design and analyze a space vector pulse width modulation (SVPWM) technology to study the motor speed using the voltage/frequency controller by using the Matlab/Simulink program, as this study analyzes the speed through two cases, in the first case, we change the reference speed with the load torque remains constant, and the other case we change the load torque with the reference speed remains constant, and in both cases, the V/f ratio must be constant, and we analyze the motor work and characteristics in both cases.

1.2 Thesis Outlines

This thesis study has included five sections, which are explained by the following points:

- Section 1: Present an introduction to this study.
- Section 2: Electric motor and the working principle of the electric motor, types of electric motors, induction motor and components it, methods for starting a three-phase induction motor, slip, power and torque in three induction motor, inverters, space vector PWM and V/f controller
- Section 3: The Mathematical analysis of the equivalent circuit for the IM, the mathematical analysis of SVPWM for an inverter of induction motor, and the simulation model represents the use of the Matlab program during using the V/f method.
- Section 4: Discuss the results of the case study using the V/f controller and for results to control the speed and torque of an induction motor when the ratio between V/f is constant in all cases.
- Section 5: Conclusions and suggestions for future works were explained in section.

2. ELECTRICAL MOTOR

2.1 Define Electric Motor

Besides, the size of the electric motors varies greatly. It could be a small device that does its job inside a wristwatch or a massive engine that powers a heavy locomotive. When mixers and generality other cookery equipment necessity small electric engines to they only need plain electrical power, trains require the utilized of bigger and extra complex engines due to the electric train motor expends sizeable electrical capacity in a low time to move (Sandeep *et al*. 2014) .

2.2 The Working Principle of the Electric Motor

Electric motors generally convert electricity into rotational motion through the properties of the phenomenon of electromagnetic induction. The operation of motors differs according to the type of electric current that the engine operates. Moreover, direct current engines are powered by joining them to a direct current supply such as batteries. The battery is connected through electrical wires with a metal coil representing the electric motor's rotating part (Siemon 1996). The battery is connected. The rotor part is through copper brushes and the electric exchanger. When the rotor section is joined to the battery, current fluxes in it, which transforms it into an electromagnet, which creates a magnetic domain about it, and the rotating part of the electric engine is surrounded by a permanent magnetic domain generated by the stator part of the engine, which causes the electromagnet to be affected by the field the surrounding magnetic field with the forces of attraction and repulsion between the poles. Thus, it is done to generate a torque that makes the coil relay in a half-turn circuitous motion. For the continuation of the rotation of this coil, it uses an electric swapper that inverts the way of the current passing out of the rotating coil, which drives to the magnates of the electromagnet inverter after every part of the cycle, which means the electromagnet go on to be affected by the forces of attraction and repulsion, and thus his rotation continued (Singh *et al*. 2014).

Additional, the precept of the running of an electric motor that works on an alternating current source formation of two prime portions, whose are the stator part and the rotating part and various the precept of direct current engines, the electric current replacement is directly fixed and is joined to the stator section of the engine, where the stator is shaped from sundry conductive electrical circles that be an electromagnet when joined to an AC, producing a magnetic domain about them, while driving to the obstetrics of an inductive electric current such comes at the closes of the mineral coil that appears the revolving section that alternates inside the stator domain. This actuated current creates an attractive domain, another at the coil, and influences by the attractive stator domain. It produces torque because of the substitute forces of gravitation and disharmony between the two magnetic fields (Zimmer 2000).

2.3 Types of Electric Motors

The main purpose for the pluralism of motor kinds is such no engine ability be considered a perfect all loaders, operations in each situation, gathering every requirement, with reasonable price and operating costs it is low and requires little maintenance. Accordingly, every engine that is manufactured has specific characteristics and advantages, and disadvantages that differ from one type to another (Hartono *et al*. 2019).

Electric motors are divided into two main types according to the type of current:

1- DC motor

2- AC motor

2.3.1 Direct current motor

It is used while the load needs to work at different speeds and needs elevation starting torque. The best type of engine which velocity ability be monitored efficiently and accurately with top allergy and a great area of variable velocity are DC motors.

DC motors are also characterized by being given a large starting torque compared to other types, where they may reach five times the full load torque. Moreover, there are disadvantages to DC motors are their high price compared to the rest of the other types, they need frequent maintenance and the starting current is very high compared to the rest of the types, reaching 20 times the current full load (Umashankar *et al*. 2016).

2.3.2 Alternative current motors

They are motors that depend on alternating current during their work and are classified according to the following. The number of feeding phases, according to the structure and according to the properties.

Alternating current motors (AC motors) are categorized in conformity to the number of phases into single-phase motors and 3-phase engines. In addition, AC motors are categorized conformity to the number of the structure into short-circuited motors (squirrel cage) and twisted-circuit motors (with slip-on). Likewise, AC motors are categorized conformity to properties into asynchronous motors and synchronous motors (Divyam *et al*. 2020).

Moreover, AC motors are of several types that satisfy simple use, such as in household uses, such as dusters, hairdryers, washing machine motors, fans, etc. These work with an average AC voltage of 110 or 220 volts, including the big ones used to operate factory machinery or run public transport metro and electric trains that speed reach 350 kilometers per hour. These large motors run at much higher voltages up to 3000 volts.

Furthermore, electric motors can be classified as shown in Figure 2.1.

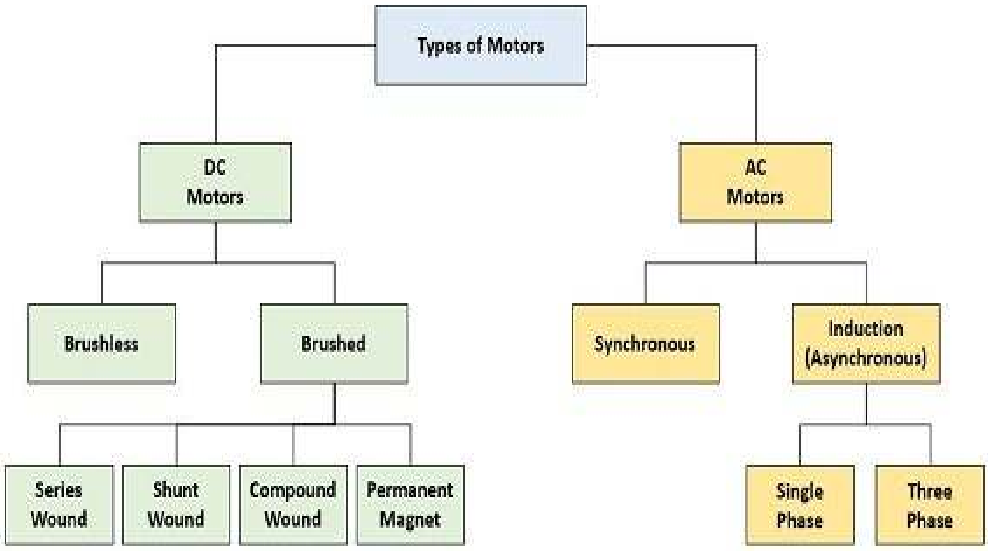

Figure 2.1 Types of motors

2.4 Induction Motor

An induction motor (IM) or it can be called an asynchronous engine is support by an AC engine through that the electrical current inside the rotor demanded to source contortion is getting through magnetism induction associated in IM will thus become produced whilst not electrical joins to the rotor. Support in IM rotor maybe each hurt isolate or squirrel-cage sort. Three-phase IM from kind squirrel-cage region unity broad utilized as manufacturing leads as an outcome of their self-running, credible, and frugally (Lehuy 2001). Single-phase IM region unity is utilized widely for short hundreds, like manage devices such as fans. Although historically used at fixed velocity employ, the IMs region unity cumulatively obtaining utilized for changing-frequency drives (VFD) at change velocity employ. VFDs provide appointed vital capacity provisions probabilities for situated and possibility IM in changeful-torque pitch fan, and mechanical equipment pregnancy implementations. Squirrel-cage IM region unity scarcely broad applied at every constant velocity, and (VFD) implementations (Hartono *et al*. 2019).

In addition, an AC flows from the fixed side object connected to an alternating voltage supply, and the current comes during the stator windings that differ in the number of poles from one motor to another, and when the alternating current passes through the coil, an alternating magnetic flux is created according to Faraday's law. This flux picks site in the magnetic loop which is formed between the rotor and the stator - since yonder is no electrical join between the rotor and the stator and while a magnetic flux comes in the furls of the rotor end, an electric current is stimulated in the rotor loop according to Faraday's law, resulting in the motion of current and the flux resulting in a revolving magnetic domain rotates the secondary tip (Divyam *et al*. 2020). Induction engines can be classified according to the feeding phases, as shown in Figure 2.2.

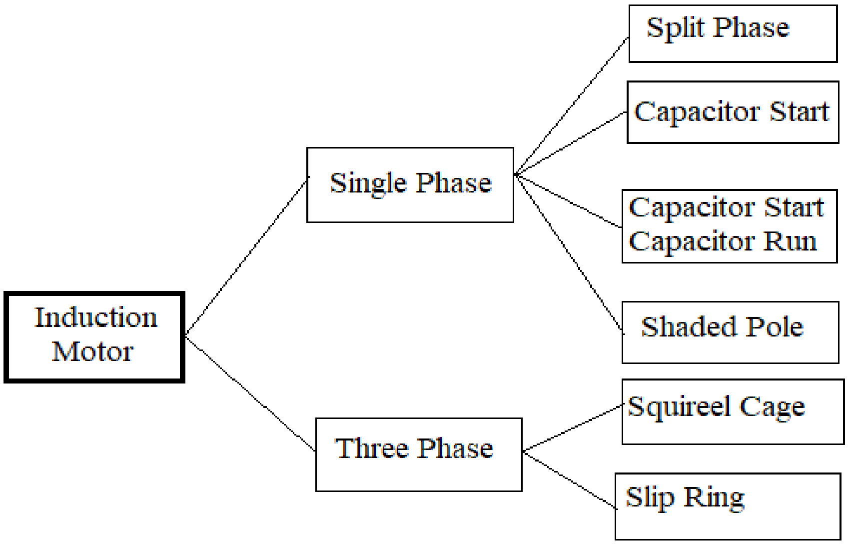

Figure 2.2 Classifications of the induction motor

2.4.1 Single Phase Induction Motor

This type of motor takes advantage of the average current found in homes (voltage 110 volts or 220 volts) to operate the usual daily machines, as it is characterized by high rotation speed and small size. This kind of electric engine is utilized to power washing equipment and dust extractors to run electric fans, hairdryers, and other simple devices used in manual factories. Besides, it initially produces strong torque currency, and its rotation speed can be changed by a frequency converter, and these motors can operate with electric power up to 3000 watts .Figure 2.3 represents the internal parts of a single-phase motor (Ferdiansyah *et al*. 2018).

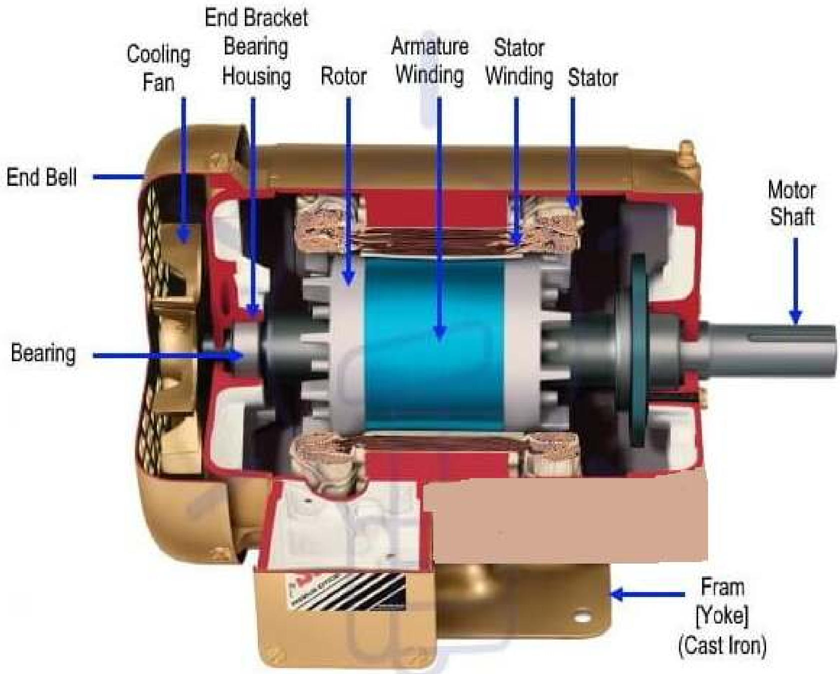

Figure 2.3 Construction of single phase induction motor (Ibrahim Shahl 2008)

2.4.2 Three phase induction motor

The three-phase IM is considered the most widespread in the scientist of industry and this has advantages such as durability and simplicity in installation, its low price compared to other motors, it does not need maintenance, it is used to get constant or variable speeds with high efficiency, the possibility of designing with horsepower capacities of approximately ten thousand horses and does not require current for the field as in motors the other (Hartono *et al*. 2019).

In addition, the disadvantages of the starter current of this motor are high, ranging between 5-7 times the whole load current, and the power factor is low at light loads.

Therefore, the advantages of these motors outweigh their disadvantages in most industrial applications, as it was recently found that electronic control methods have led to overcoming these defects, and induction motors are called this name because the efforts and currents generated in the files of the rotating organ are generated by induction from the effect of alternating currents in stator windings, just like in transformers, an induction motor can be trapped in a rotating transformer, its primary windings static, and secondary windings for rotating motion (Ferdiansyah *et al*. 2018). Figure 2.4 represents the internal parts of a three-phase motor.

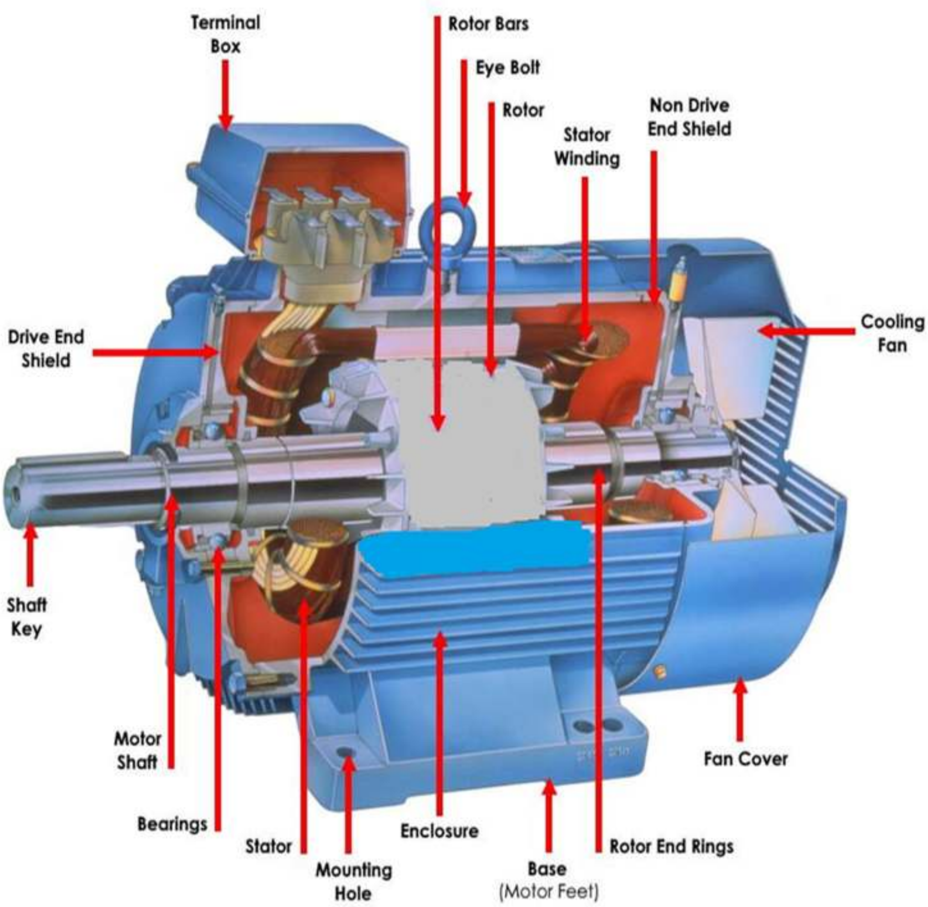

Figure 2.4 Construction of a 3-phase induction motor (Ibrahim Shah 2008)

2.5 Components of an Induction Motor

The 3-phase engine consists of two major members which are the stator and the rotor.

2.5.1 The stator

The stator consists of an external iron cylinder composed of compact strips of magnetic iron ranging in thickness from 0.3 mm to 0.6 mm and isolated from each other by an electrical insulator such as oil or paper, that they form with each other the cylindrical body. When manufacturing slides, it is taken into account in their formation to have many ducts inside the cylinder to install the files. The goal of making the stator in this method is to reduce the eddy currents that raise the temperature of the iron due to the iron's exposure to the changing magnetic field inside the motor, and it is considered wasted energy that is not used. After manufacturing the stator in this way, it is divided into the required number of electrodes, and then the windings of each phase are installed in its conduits so that each phase is separated from another 120 degrees (angle see phase shift). At the end of the process of downloading the coils in the sewers, we may have three coils in the stator, each of which has two ends, through which the stator is supplied with alternating current, either a star connection or a delta connection (Aspalli *et al*. 2011).
Generally, the stator is composed of the outer frame, the stator chips, and the stator coils.

2.5.1.1 External frame

It is made of cast iron (steel) or aluminum with pitches on its outside flatten that coldish the windings through the air blown by the cooling propeller. The structure is used to load the core-forming wafers and to install the side spoilers and the connecting plate box, as shown in Figure 2.5.

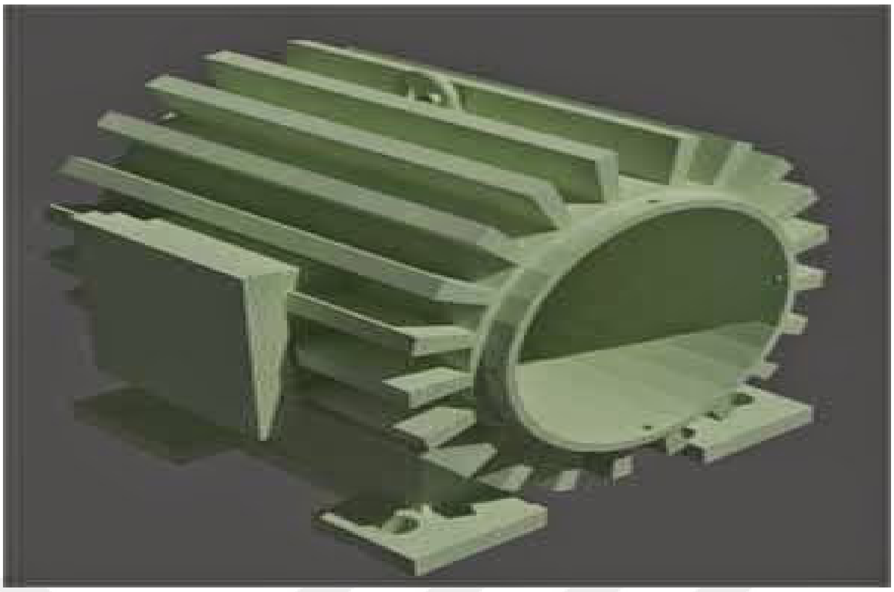

Figure 2.5 Structure frame (Shafi 2009)

2.5.1.2 Core stator

It is made of silicon steel sheets (to reduce the losses of magnetic retardation) and isolated from each other with a varnish material (to reduce the losses of cyclonic currents) and it is formed in the form of a slotted ring with its inner surroundings, as shown in Figure 2.6.

Figure 2.6 Stator chips (Shafi 2009)

2.5.1.3 Stator windings

It is made of copper wires insulated with varnish, wrapped on a special grinder with size and the numeral of turns commensurate with the power of the engine and linked to the voltage and current passing through it as shown in Figure 2.7. The method of connecting the stator windings is divided into two parts (Laithwaite 1975).

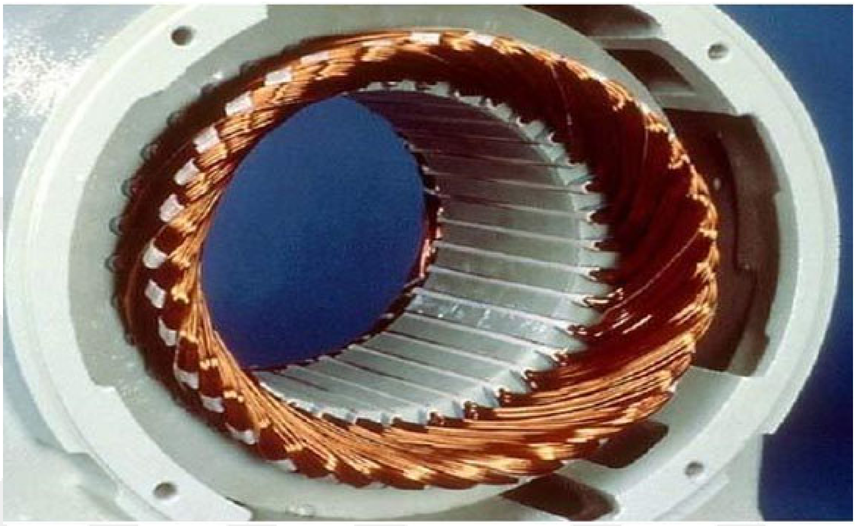

Figure 2.7 Stator windings

The first method to connect stator coil is star connection where the three ends are connected in one point and connect the three beginnings to the source, as shows in Figure 2.8.

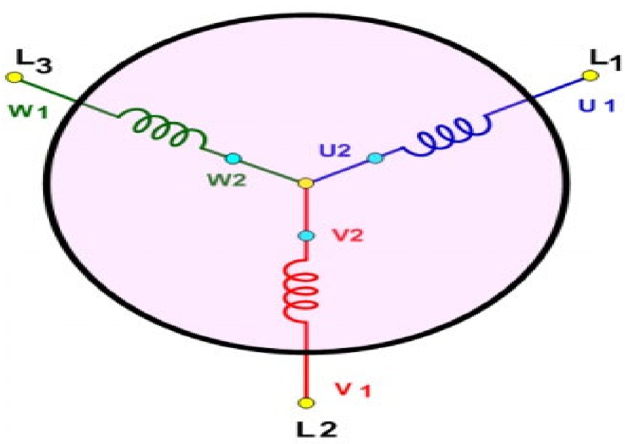

Figure 2.8 Connection stator coil with star method

The second method to connection stator coil is delta connection where the end of the first face connects with the beginning of the second face, the end of the second face the beginning of the third face, and the end of the third face the beginning of the first face, as shown in the Figure 2.9.

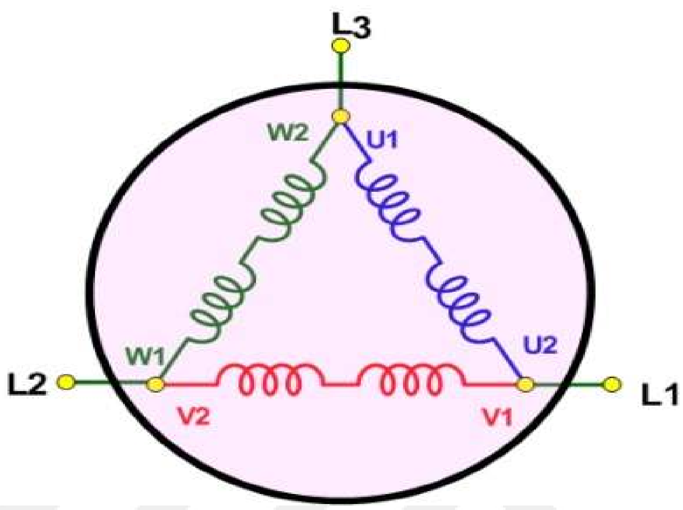

Figure 2.9 Connection stator coil with delta method

2.5.2 The rotor

Two types of the rotor are different in composition and are similar in electrical properties, and an electric motor is usually called by the name of its rotor to distinguish between its two types, which are wound rotor motor (slip rings motor) and squirrel cage rotor motor.

2.5.2.1 Wound rotor

The slip rings rotor shall be composed of compact strips of magnetic iron, and the slats are isolated from each other, as in the stator assembly. It is installed on the motor shaft and engraved in it many ducts to install the rotor coils. The rotor is divided into many piles equal to the stator poles, and the sewers in each pole are divided into three sections, each section in which the coils of one of the three phases are installed, and the coils are connected in a star shape and their ends are connected to the slip rings (electrical exchanger) using sliding rings. Through carbon brushes tangent to the sliding rings during rotation, the rotor wraps are joined to the electric current from the outside. This can start the rotation of the motor or regulate its speed. This type of motor is characterized by the ability to change its operating properties by connecting the rotor windings with a variable outer resistance because controls the torque and thus the engine speed.

2.5.2.2 Squirrel cage rotor

The squirrel-cage rotor is the same as the sliding-ring rotor in terms of mechanical structure, but instead of coils in the ducts, copper or aluminum rods are placed in the slat ducts in the form of the cage. These rods are connected on the two sides of the rotor by two rings of copper or aluminum. This cage type does not divide into a specific number of poles, but can automatically adapt to the number of poles and phases of the stator, and it has no slip rings and therefore cannot be linked to an external circuit and its operation properties cannot be controlled, because it rotates under the effect of magnetic induction from the stator (Therib 2017).

2.6 Rotating Magnetic Field

Since the stator windings are connected either in the form of a star or a delta, and between each coil there is an angularity of 120 degrees while those turns are joined to a 3-phase voltage supply, alternating currents will pass in these windings, between each current and the angle of 120 degrees, and will create in the air gap a regular rotor magnetic domain is between the rotor and stator. This domain rotates at a velocity called the synchronous velocity and the intensity of this magnetic domain is straight relative to the phase current go by during the stator and the number of turns in the stator under each pole (Hartono *et al*. 2019).

The synchronous velocity is computed from the below-shown with Equation (2.1):

$$N_s = \frac{120\,f}{p} \tag{2.1}$$

Where N_s is the synchronous velocity and mensuration in rpm, (f) is the frequency of the stator, and (p) is the number poles.

In addition, the intensity of this magnetic domain is straight commensurate to the face current go by during the stator and the numeral of wounding in the stator member under each pole is finding from the Equation (2.2):

$$F_s = n_s . I_s \tag{2.2}$$

Where (F_s) is the magnetic domain intensity, (n_s) is the number of stator mutations for each pole, and (I_s) the effective value of the present current in the stator.

2.7 The Principle of Operation of an Induction Motor

When the stator terminals are joined for the voltage source, it will make a revolving magnetic domain, this rotating magnetic field will generate an electric motive force in an electric conductor that is within a range of influence according to the phenomenon of electromagnetic induction, and while the rotor falls inside the impact of this revolving magnetic domain, it will arise in its conductors a three-phase electric momentum, and since the rotor conductors are restricted at both ends, three-phase currents will pass between each face of 120 degrees, and then another rotating magnetic domain will be generated at the air gap as a score of the crossing of 3-phase currents in the conductors of the rotor. In this case, we have two magnetic fields, the first rotation is created through the stator and rotates at the synchronous velocity N_s and the second is produced by the rotor and rotates at (N_s – N) with respect to the rotor - where N is the rotor velocity - and rotates at the synchronous velocity N_s with respect to the stator and since these two magnetic fields(Barrero *et al*. 2014). They are revolving with the same velocity and trend, then an active torque will be produced on the rotor leading to its turning in the same trend and turning on the two domains, according to the precept of torque production, as shown in Figure 2.10, this torque is directly relative to the intensity of the two fields and the sine of the angle between them according to the Equation (2.3)

$$T \propto F_s \cdot F_r \cdot \sin(\delta_{sr}) \qquad (2.3)$$

Where T is the torque, (F_s) is the density of the stator for the magnetic domain, (F_r) is the density of the rotor for the magnetic domain and $\sin(\delta_{sr})$ is the angle between the two domains.

The rotor after that begins with fast, the velocity of insinuation of its conductors to sever the lines of the rotating magnetic field will lower as the rotor velocity raise layer for the following Equation (2.4).

$$N_F = N_s - N \qquad (2.4)$$

Where N_F is the severing velocity of the magnetic domain bars of the rotor bars.

Thus, the electromotive force generated in the rotor conductors will decrease with the increase in the rotor speed because the electromotive force generated due to electromagnetic induction is directly proportional to the prorated speed between the jointer and the domain it is exposed. Consequently, the value of the currents passing in the conductors of the rotor will decrease and consequently the intensity of the magnetic domain generated by them will decrease, and then the torque affecting the rotor will decrease, and so on until the rotor speed reaches a velocity near to the synchronous velocity. When the rotor velocity amounts to near to the synchronous velocity, the currents generated in the rotor conductors are small, and thus the magnetic field arising from them weakens, which leads to a reduces in the torque effect on the rotor, and when the rotor velocity stabilizes, the torque effect on the rotor is egalitarian to the spirant power that the rotor is exposed (Soni *et al*. 2013).

Moreover, when the motor is loaded, the rotor velocity decreases and this results in a rise in the speed of the magnetic domain cutting of the rotor conductors, which leads to an increase in the values of the currents passing through its conductors and thus a rise in the intensity of the field arising from them and then increasing the torque affecting the rotor, then the velocity of the rotor stabilizes at the speed and then the torque affecting it is equal to the torque of the load imposed on it (Swamy and Kumar 2008), as shown in Figure 2.10.

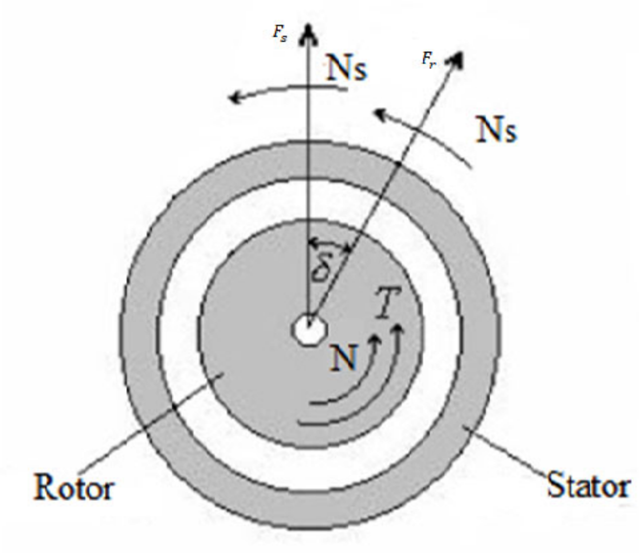

Figure 2.10 Relation between field and speed (Ibrahim Shahl 2008)

2.8 Methods for Starting a Three-Phase Induction Motor

Operation or starting of three-phase IM there are several methods.

2.8.1 Direct on line

One of the cons of three-phase induction motors is that they draw a very high starting current from the electrical grid up to 8 times the nominal starting current (In) and this affects greatly, especially if the network is feeding other loads, the high starting current causes a voltage drop grid (during operation period), this affects other carries (Kamini *et al*. 2014).

The direct online method can be used with three-phase induction motors, and it is recommended that the motor power to be started in this way does not exceed 5kw.

From the features of the direct online method single of the easiest and most economical methods, ease of application, work, and maintenance, its control circuit is very simple, ease of understanding and fault detection, torque ratio at takeoff 100% and requires only one triple cable from the board to motor.

In addition, the cons of this method peak starting current causes shortening of motor life. Causing a voltage drop at take-off that affects other equipment connected to the supply line, large starting torque may not be important to the load causing stress on the mechanical portions of the engine, and the immediate line method is not suitable for applications influenced by rising currents such as mechanical stairs and elevators (Mohamed *et al*. 2014).

2.8.2 Starting star - delta

This method relies on reducing the voltage source to the engine from starting to connect the motor windings on the form of the star. Thus, the beginning current is miniature to one-tertiary of the current if the motor is started directly.

The advantage of this method is the low cost of this method, the motor in this way runs for unlimited hours, elements of this method require little space, and the starting current of this method is reduced by one-third (Ferreira *et al*. 2014).

Moreover, from the cons of the star-delta method starting with the (star-delta) method reduces the current to a third but also reduces the torque to a third. The motor terminals in this method require two cables from the motor to the board, this method provides a starting torque of 33%. If the pregnancy joint to the engine requires high torque during startup, high pressure will form when converting from star to delta, which may cause the system to break, motors that require starting torque greater than 50% of the engine torque are not suitable for starting with star-delta and whether the engine is loaded with a very large load, thither shall not produce torque for the engine to reach sufficient speed for delta (Sarkar 2006).

2.8.3 Reducing voltage

Reducing the voltage applied to the stator circuitous driving to a lower starting current at the same rate as the voltage lessening. When utilizing resistors, a group of resistors is jointed in series with the stator circuitous during the first start-up period to reduce the value of the applied voltage (Zhou *et al*. 2013). The value of the current decreases by the same as the decrease in the voltage itself, and the value of torque and current ability be replaced by variable the amount of the resistors, so the starting here is smooth.

In addition, the reducing voltage method is used to start machines with an increased load torque, and the values of these resistors range from parts of an ohm to several ohms, and some of them are immersed in oil to cool them due to the passage of starting currents in them. Once the engine speed is stabilized, the resistors are eliminated (Zhou *et al*. 2013).

2.8.4 Soft starter

Using the soft starter method to find solutions to the disadvantage found in the reducing voltage methods. They are mainly manufactured based on thyristors, which regulate the voltage source to the engine and the monitoring circuit that controls the action of these thyristors. Inside it, there are conduits and a fan that dissipates heat. It also contains transformers to measure the current.

Basically, a soft starter does not change the current or speed as in a speed driver, but rather raises the voltage utilized to the engine from the prime amount to the full voltage, and both torque and voltage will accelerate, this leads to the machine's acceleration (Zenginobuz *et al*. 2001).

One of the advantages of a soft starter is that it adjusts the torque to the value that the machine needs, and it also reduces the stress on the equipment and thus the need for maintenance is reduced, and the soft starter can make a soft starter (Antonino *et al*. 2014).

2.9 Slip in Induction Motor

The rotor in induction electric motors rotates at a speed less than the velocity of the magnetic domain because if it revolves at the same velocity, there will be no (EMF) generated in its coils due to the lack of proportional velocity between these coils and the rotating magnetic domain. The difference between these two speeds is called the sliding speed (Lu *et al*. 2013).

As the electric motor rotates at the highest speed if the engine is running without load and the slip, in this case, is in the lowest cases and the slip increases to reach its highest value when the engine is running at full load and there are some terms related to the subject of slip, the slip speed N Slip (Yanxin *et al*. 2013), which is the resulting speed difference Equation (2.5) formulates between the velocity of the revolving magnetic domain (synchronization speed) inside the stator and it as (N_s) and the actual speed of the rotor (N_r) (Echavarria *et al*. 1995).

$$N_{Slip} = N_s - N_r \tag{2.5}$$

Equation (2.6) and Equation (2.7) use for calculation of the slip coefficient is the percentage between the velocity of skid and the velocity of the magnetic domain (synchronization speed), where:

$$S = \frac{(Ns - Nr)}{Ns} \tag{2.6}$$

$$S = \left(\frac{N_s - N_r}{N_s}\right).100\% \tag{2.7}$$

2.10 Power in Three-Phase Induction Motor

A three-phase IM is usually described as a rotating transformer and the input is electrical power in the primary windings (stator) form of voltages and currents three-phase and the produce is electrical energy possessed from the secondary windings of the converter, whilst in an induction motor, the secondary windings are shortened and thus do not give electrical energy but give mechanical energy (Dinakaran 2015).

It appears on the revolving column, a Figure 2.11 showing the flow diagram of the power inside the induction motor, where P_1 it represents the electrical energy pulled from the source, and P_2 the mechanical energy output (Wang *et al*. 2013).

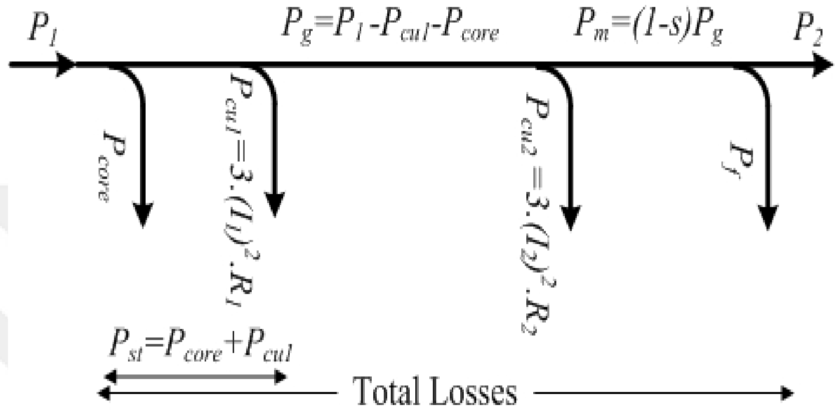

Figure 2.11 Power flow inside a three-phase induction motor

The inductive engine from the 3-phase source takes the total power, which is equal to

$$P_1 = 3V_1.I_1 . \cos \emptyset \qquad (2.8)$$

In Equation (2.8), V_1 is the stator voltage, I_1 is the stator current, and $\emptyset$ the angle between stator current and stator voltage.

Furthermore, the missing stator coils are dissipated (P_{cu1}) with copper in the resistance(R_1) of the stator in the form of heat, and it is calculated from the equation (2.9). It is also dissipated at the same time total iron losses the motor (P_{core}) due to the presence of eddy currents and the phenomenon of magnetic retardation in the stator and the iron losses of the rotor are very small due to the decrease in the frequency value is when the slip is very small at full load (Emadi *et al*. 2008).

Sum P_{cu1} with P_{core}, we obtain the called stator losses as in Equation (2.10). This losses power is represented by resistance R_c in the equivalent circuit.

$$P_{cu1} = 3(\mathrm{I}_1)^2 . R_1 \quad (2.9)$$

$$P_{st} = P_{cu1} + P_{core} \quad (2.10)$$

The remaining part of the input power P_1 after subtraction P_{st} will transmit during the air gap to the constant magnetic field and it is called the power of the air gap and represent by a symbol P_g .

$$P_g = P_1 - P_{st} \quad (2.11)$$

Moreover, can be calculated P_g also from the Equation (2.12), as:

$$P_g = 3(I_2{'})^2 . (\frac{R_2{'}}{S}) \quad (2.12)$$

The input power to the rotor P_g will lose part of it in the resistance of the rotor windings in the form of heat. It is called the copper losses of the rotor member P_{cu2} and is calculated from the following equation (Dinakaran 2015).

$$P_{cu2} = 3(I_2{'})^2 . R_2{'} \quad (2.13)$$

The remained from input power to rotor converter from electrical energy to mechanical energy, the called mechanical energy generated and it by the symbol P_m , the calculated from the following equation:

$$P_m = P_g - P_{cu2} \quad (2.14)$$

The resistance ($R_2'\left(\frac{1-S}{S}\right)$) in the equivalent circuit is that which represents the generated mechanical power (Wong *et al*. 1997), and thus the generated mechanical power can also be calculated through the Equation (2.15)

$$P_m = 3\,(I_2')^2 . R_2' . \left(\frac{1-S}{S}\right) \quad (2.15)$$

The generated mechanical power will dissipate part of it due to the friction that the rotor is exposed to with the air and the rotation axes, these friction losses are symbolized by a symbol P_f, and therefore the mechanical power output P_2 (useful mechanical power) is the remaining part of the mechanical power generated after deducting the power dissipated due to friction as follows:

$$P_2 = P_m - P_f \quad (2.16)$$

2.11 Torque in Three-Phase Induction Motor

Torque is defined as the force that exerts a torsional effect on an object resulting in the rotation of that body around a focus and measured in (Nm.) (Kidouche *et al*. 2013).

The total torque in the induction motor is produced through the revolving magnetic domain at the synchronous speed Ns, which is obtained by dividing it P_g on ω_s in the Equation (2.17).

The same total torque is created on the rotor which rotates speedily N due to mechanical power P_m, and we get it by dividing it P_m on ω as in the Equation (2.18).

$$T = \frac{P_g}{\omega_s} \tag{2.17}$$

$$T = \frac{P_m}{\omega} \tag{2.18}$$

Where ω_s the angular speed of the revolving magnetic field and ω the angular speed of the rotor (Riveros *et al*. 2013).

$$\omega_s = \frac{2\,\pi\,.\,N_s}{60} \tag{2.19}$$

$$\omega = \frac{2\,\pi\,.N}{60} \tag{2.20}$$

By offsetting an Equation (2.12) and Equation (2.19) into the Equation (2.17), we get the Equation (2.21).

$$T = K\,(\,I_2{}'\,)^2.\,(\frac{R_2{}'}{S}) \tag{2.21}$$

Where,

$$K = \frac{90}{\pi.N_s} \tag{2.22}$$

$$I_2{}' = \frac{V_1}{Z_{eq}} = \frac{V_1}{\sqrt{(\,R1+\frac{R_2{}'}{S})^2+(X_{eq})^2}} \tag{2.23}$$

By substituted the Equation (2.23) into the Equation (2.21) get on:

$$T = K\left(\frac{V_1}{\left(R1+\frac{R_2{}'}{S}\right)^2+(X_{eq})^2}\right).\left(\frac{R_2{}'}{S}\right) \tag{2.24}$$

Equation (2.24) represents the relationship between torque and slip, including calculating torque at any value of a slip and therefore at any value of velocity (Sundararaju *et al.* 2017). When drawing the relationship between torque and slip or between torque and velocity from the equation, we obtain the curve shown in Figure 2.12.

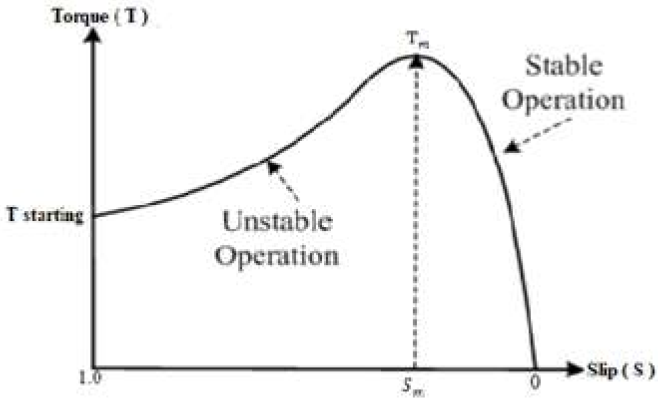

Figure 2.12 Torque and slip curve for an induction motor

The curve of the relationship between torque and slip in Figure 2.12 is divided into two different parts, from S = 0 to S = S_m. The torque increases with the increase in the slip value, while the torque exerted by the motor decreases from S = S_m. to S = 1, so the motor has balanced operating properties in the first part, while the properties of an unbalanced batch are in the second part. The inevitable result of the existence of two different regions in the properties of the engine, one of which has the property of equilibrium and is absent in the other. Therefore, we must make sure that the engine operation is confined to the equilibrium zone, so it does not move to the other region except under conditions beyond control (Ansari *et al.* 2010).

Usually, the full load torque is approximately equal to half of the engine's maximum torque, provided that it does not exceed the starting torque, and if the load torque is greater than the starting torque, the motor cannot start rotating so the motor must be started without load and after it reaches the balanced operating area, the load is added.

The total torque (T) consists of the useful torque (T_u) and the torque of the mechanical losses (T_f). The useful torque is fully utilized in the mechanical form while the waste is wasted (Sundararaju *et al*. 2017). The useful torque can be obtained by dividing the output power by P_2 on ω as in the Equation (2.25).

$$T_u = \frac{P_2}{\omega} = \frac{P_2}{2\,\pi\,n/60} \tag{2.25}$$

Additional, Figure 2.13 shown the typical torque-speed particulars of an IM. The X-axis offers velocity and skids whilst the Y-axis offers torque and current. When the engine is run, it pulls a much big current to the regulation of seven times the estimated current, which is an outcome of the stator and rotor outflow. Also, the beginning torque is about 1.5 times the estimated amount for the engine. As the velocity rise, the current lessens a little and then declines significantly while the velocity range is near to 80% of the estimated velocity. At the foundation velocity, the estimated current fluxes in the engine and estimated torque are received. Moreover, at foundation velocity, if the load exceeds the estimated torque amount, the velocity lowering, and the skids rise at 80% of the synchronous velocity, the load accretion up to 2.5 times the rated torque, that is called collapse torque. Increasing the pregnancy further causes the torque to fall rapidly and the engine stalls.

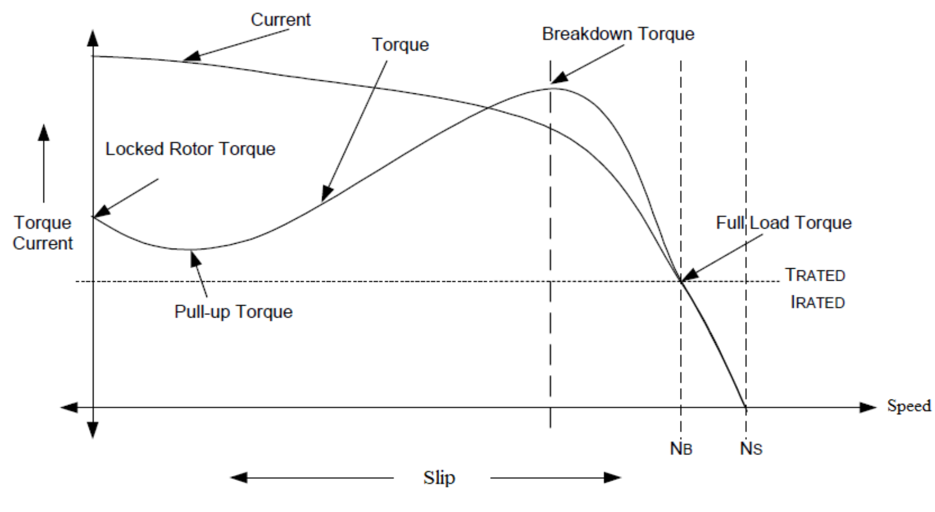

Figure 2.13 Torque and speed curves (Kamini *et al.* 2014)

2.12 Inverters

Inverters convert a constant current of good constant value into an alternating current that can be controlled, there are various modes of monitoring the produce voltage value of the inverter, such as controlling the constant voltage value or controlling the output AC voltage in the pulse width mode while the frequency is controlled by control of the time cycle of the contact process and the separation of the used power electronics components (Soni and Gupta 2013).

Inverters are utilized in a big number of industrial implementations such as uninterruptible power supplies, speed control instant messaging, and synchronous motors, which are used in industrial applications requiring variable speeds. Transformers can be divided according to the type of output voltage into single-phase transformers and 3-phase transformers. To control the speed of 3-phase IMs, inverters are utilized to monitoring the voltage supplied to the stator, monitoring the frequency, or control the voltage and frequency together (Birbir *et al*., 2008). This is done by using several types of inverters such as a 3-phase inverter with a constant good applied and a 3-phase inverter for a variable-width pulse (Nogay *et al*. 2008).

2.13 Space Vector Pulse Width Modulation

Multilevel inverters can produce sine voltages from separate voltage levels, and PWM implements a strategy for this function to generate sines of replacement in frequency and voltage. According to the frequency switching methods, the modulation methods of the multi-level hybrid inverter can be classified. To achieve a wide linear modulation domain much various PWM methods have been developed, and one of the development methods is minimum switching loss, less computation time, easy execution, and miniature THD in the waveform switching miniature (Casadei *et al*. 2000). To implement a strategy of the pulse with modulation (PWM) for large-scale multilevel inverters and the techniques most used are space vector PWM and sinusoidal PWM. Further, SVPWM is deemed to be the best technicality for implementing PWM as it has pros over SPWM on expressions of perfect utilize of DC bus voltage depressed ripple current, and depressing transition frequency (Hyun *et al*. 2003).

SVPWM is considered to be the best technique for implementing PWM, as it supplies s the following characteristics:
(1) Best basis output voltage.
(2) Helpful in reducing THD and it works on improving harmonic performance.
(3) Easy used and simple implements in a digital signal processor (DSP).

Additionally, SVPWM is a fast PWM method that achieves similar results to other PWM methods in a few microseconds. Defined the space vector is in a two-dimensional (2-D) level in this analysis, and the SVM is implemented on that plane. Additionally, the three-dimensional (3-D) space vector for the cascading multi-level H-bridge reflector is described in this analysis. PWM schemes are currently available in many configurations. Since all current PWM schemes are two-dimensional, they can't handle the zero-sequence portion caused by an unbalanced load. Since the generality of the SVM algorithms offered in the literature utilizes trigonometric function calculations or lookup tables, the complication and calculation of the conventional SVPWM technique increase with the numeral of reflector levels (Perales *et al.* 2003).

However, Diode-clamped inverters cannot be used with unequal DC sources developed the first 3-D space vector modulation (SVM) cascaded H-bridge inverters, which can deal with zero-sequence components induced by unbalanced loads. The 3-dimensions SVM schemes are supersets of the 2-dimensional SVM schemes and thus compatible.
Moreover, schemes for two-dimensional SVM that are widely used proposed a new optimized 3-D SVPWM (3-D SVPWM) technique, which is identical to the current 3-DSVPWM presented in and uses the same notation (Kouzou *et al*. 2009). The suggested SVPWM method determines the switching vector series that is closest to the reference vector, as well as the status intervals of each switching case, without the use of trigonometric task, research tables, calculations, or assortment system conversions a vector, can be generated using simple addition and comparison operations. Because of their low complexity and computational expense, they are ideal for use in low-cost

devices. It's worth noting that this three-dimensional SVPWM technicality ability is used on both unbalanced and balanced methods. The two-dimensional SVPWM and three-dimensional OSVPWM techniques are implemented. Each SVPWM algorithm is performed in a domain programmable portal arrangement. All simulations are produced using Matlab/Simulink. Finally, a cascaded H-bridge multilevel inverter was used to evaluate all algorithmic implementations.

2.14 Voltage/Frequency Speed Control

For the voltage/frequency (V/f) speed control of the IM, there are two ways:

1. Scalar method: the control circuit mainly takes during this method the reference velocity and the actual velocity of the engine into consideration. The implementation of this method depends on the variance between the actual velocity, the reference velocity, and the determination of the portal pulse frequency of the IGBT. The fixed V/f has been achieved utilizing a 6-pulse inverter with PWM burning. The traditional method of controlling a motor is to convert the phase voltage into a direct current. The DC has transformed again into single or 3-phase AC as each pregnancy requirement. The frequency produced voltage or together abilities be controlled through the usage of energy electronics and microcontrollers (Priyanka *et al.* 2016).

2. Space vector method: this method is called space vector modulation (SVM) technology was primarily progressing as a vector path for PWM for a 3-phase transducer. It is a large sine wave generation technology that delivers top motor voltage with less overall harmonic deformation. It grants a top produced voltage of the same DC voltage, down switching lakes, and best symmetrical performance. In general, open-loop systems utilized voltage/ frequency control whose is utilized in a great numeral of implementations wherever the primary requirement is to change the engine velocity and control the engine functional. In addition, it is easy to perform and effective from where the cost.

The pros of using V/f to control the velocity of a 3-phase IM is the following, the current demanded in the start is lower and the engine operations are large in a stable region. In-state of just operation at a basic estimated velocity, the engine ability typically works from 5% of synchronous velocity to the foundation velocity. The torque produced during the engine ability be kept fixed everywhere in this region (Ibrahim *et al*. 2013).

Additionally, we ability push the engine behind the basis velocity during growing the frequency even large. Further, the supply voltage ability is not be raised behind the estimated voltage. Therefore, only the frequency ability be growing, while drives to a lower at the torque. The factors controlling torque becomes complicated while the velocity is more top than the foundation velocity.

Moreover, by varying the motor's supply frequency according to period, we ability to monitoring the go low and acceleration of the engine (Yadav 2016).

2.15 Voltage/Frequency Control Principle

The speed of an IM is relative to the applied frequency and the numeral of poles of the engine. Which the numeral of poles is constant through manufacturing or design, the better method to change the velocity of IM is to change the display frequency. It is relative to the source voltage ratio and the apply frequency where the torque is advanced by an induction motor. Figure 2.14 show that, the torque ability is protected fixed over the velocity area through change voltage and frequency while conservation the proportion constant (Soni *et al*. 2013).

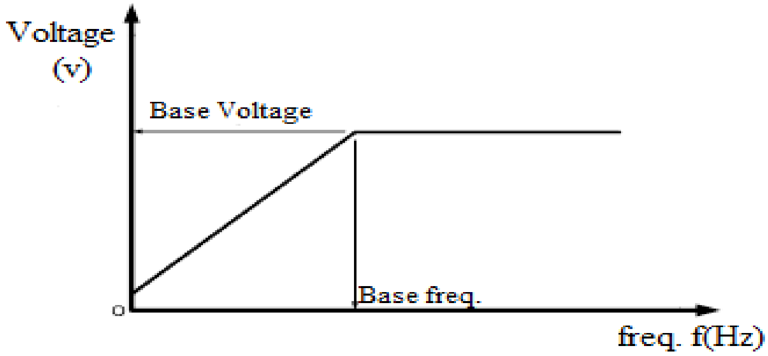

Figure 2.14 Voltage-frequency control (Soni and Gupta 2013)

However, the difference in velocity, the torque-speed characteristics of the control V/f detect that the dependent start current requirements are minimum. The motor stabilized running area is raised. In-state of just operating at its rated basis velocity, the engine's ability typically operation from 5% of synchronous velocity (N_S) to the prime velocity. The torque produced via the engine ability be saving constantly over this area. In core velocity, the frequency, and voltage arriving at the estimated amounts. We ability push the engine behind the basis velocity by raised the frequency even more. However, the supply voltage ability not be raised behind the estimated voltage. Therefore, the frequency ability is raised only, resulting in a decrease in the torque (Soni *et al*. 2013).

The deceleration and acceleration of the engine's ability be monitoring from the variation in the applied frequency of the engine with the estimate to time. A diversity of IMs is changed and currently used in the domain of manufacturing implementations. Single-phase IMs are vastly utilized, due to elevation performance, ease, and power. They are utilized in household types of tools, such as refrigerators, fans, airtight compressors, pumps, air conditioners, and washing machines. Likewise, in several industrial implementations (Yadav 2016).

3. SIMULATION OF THREE-PHASE INDUCTION MOTOR

3.1 Equipollent Circuit of the Induction Motor

The polyphaser IM ability be given as a polyphaser converter the EMF produced through the rotor currents is rotating at a synchronous velocity prorated to the stator winding, it motivates a source frequency voltage solely as in a normal transformer (Yaseen *et al*. 2018). As shown in Figure 3.1.

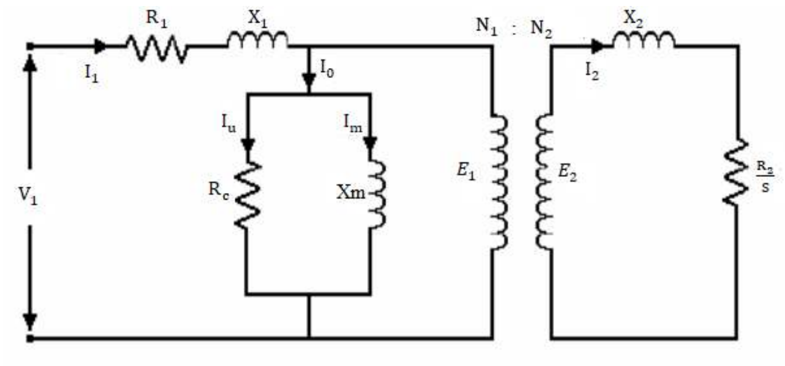

Figure 3.1 General equipollent circuit of induction motor

Where V_1 is the applied voltage, R_1stator resistor, $X_1$the stator reactance (influx which does not connect with the rotor and air gap), magnetizing reactance demanded to passed the air gap is symbolized X_m and core leakages (eddy and hysteresis current) through R_c , I_1 stator current and K_{w1} stator winding coefficient.

Whereof N_1 and N_2 in the ideal converter is represented numbers turns respectively the air gap. For the rotor side, where R_2 is the rotor resistance and X_2 is the rotor reactance Affected emf from during the slip (as the rotor increase velocity, slip lessens, and lower emf is produced), K_{w2} rotor winding coefficient, I_2 rotor current , $\emptyset_m$ maximum phase flow, and I_m magnetization current.

Moreover, can be calculated leakage reactance as in Equation (3.1).

$$x = 2\pi f . L \tag{3.1}$$

In addition, can be determine rotor emf at S=1

$$E_b = 4.44 f . N_2 . K_{w2} . \emptyset_m \tag{3.2}$$

Also,

$$E_1 = 4.44 f . N_1 . K_{w1} . \emptyset_m \tag{3.3}$$

$$E_r = s . E_b \tag{3.4}$$

Where, E_1 is the stator emf and E_r is the rotor emf.

$$I_0 = I_u + I_m \tag{3.5}$$

Where, I_0 excitation current and $I_u =$ core - loss current.

The secondary variables and parameters of the model general equipollent loop of the IM ability be mention as the elementary. For suitability, this is done by adding primes to the symbols for the secondary current, voltage leakage reactance (Pustovetov 2017), and resistance as shown in Figure 3.2.

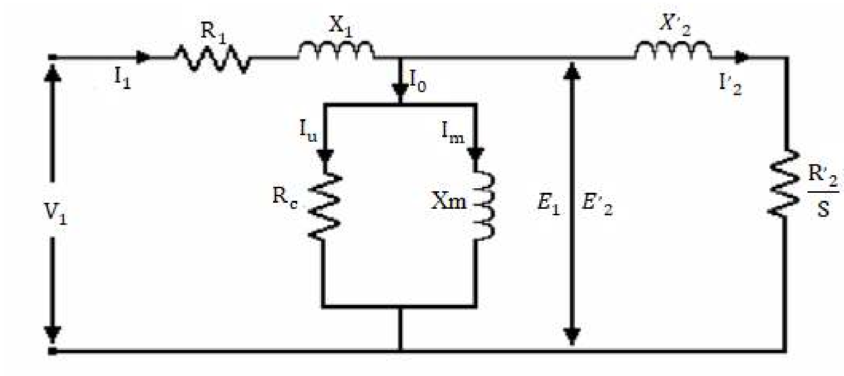

Figure 3.2 Parameter of rotor mention to the primary

$$E'_2 = (\frac{N_1}{N_2}) \, . E_2 \tag{3.6}$$

$$E'_2 = X_2 \, . (\frac{N_1}{N_2})^2 \tag{3.7}$$

$$(\frac{R'_2}{S}) = (\frac{R_2}{S}) \, . (\frac{N_1}{N_2})^2 \tag{3.8}$$

$$I'_2 = I_2 \, . (\frac{N_2}{N_1})^2 \tag{3.9}$$

Thus, we can rewrite $(\frac{R'_2}{S})$ into the equation (3.10) and the below in Figure 3.3.

$$(\frac{R'_2}{S}) = R'_2 + R'_2 \, . (\frac{1-S}{S}) \tag{3.10}$$

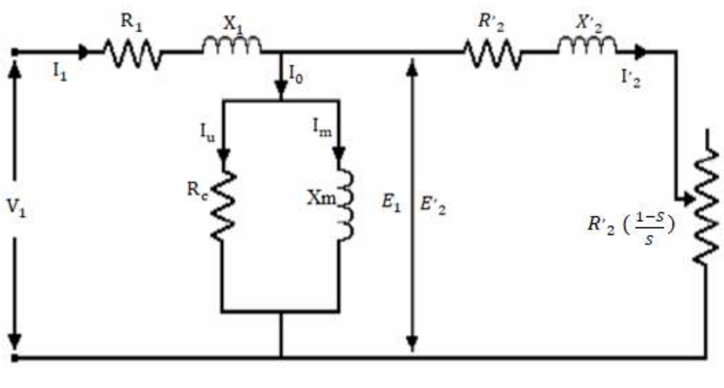

Figure 3.3 Equipollent circuit of the IM

The convergent circuit is the foundation in the presumption which $E_1 = E_2' = V_1$. In the up loop, the lone ingredient which counts on the slip is resistance. While remaining the other quantities are fixed.

$$Z_{eq.} = \left(R_1 + \frac{R'_2}{S} \right) + j\left(X_1 + X'_2 \right) \tag{3.11}$$

Where $Z_{eq.}$ represent equivalent impedance for the equivalent circuit of the IM.

$$I'_2 = V_1 / Z_{eq.} \tag{3.12}$$

Putting the value of $Z_{eq.}$ from the Equation (3.11) in the Equation (3.12) we get:

$$I'_2 = \frac{V_1}{\left(R_1 + \frac{R'_2}{S} \right) + j\left(X_1 + X'_2 \right)} \tag{3.13}$$

In the induction motor the stator core loss subsists as long as the engine is connected to a source, the rotor core loss subsists when the slip is any value other than zero, and the wind age and friction losses exist when the engine rotates. The wind age and friction losses are significantly major than others, it is common to group each of them as rotational losses and remove Rm from the circuit model. This is suitable since the no-load power is the total of these losses other than the small copper losses, and normally it is not possible to separate the core loss from the mechanical loss (Husham and Ahmed 2015). Naturally, this introduces a small error in calculated values of gap power, but this error is quite measly when this is done, the equipollent loop seems as shown in Figure 3.4.

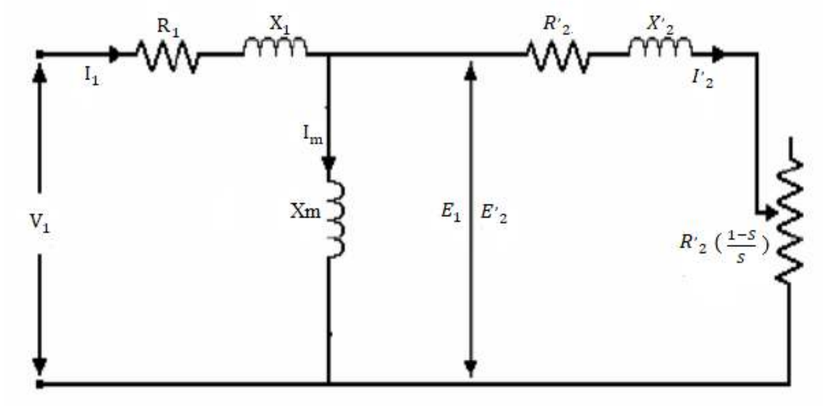

Figure 3.4 Approximate equipollent loop of induction motor

3.2 Svpwm Principle and Voltage Supply Inverter

The 3-phase voltage source inverter (VSI) contents from six switches for three legs as shown in Figure 3.5. It will be utilized two appear to back joined semiconductors at each switch of the inverter. Moreover, but at while two switches, one will be a diode for protection and the second will be a controllable apparatus. The voltage waveforms for each 3- phase are shown in Figure 3.6. It is monitored while the status of first inverter leg variations after an interval of 60 degrees and then its states remain fixed for the 60-degree duration. Therefore, the leg voltage will have 6 distinguished and separated amounts of 360 degrees during one cycle (Padmathil *et al*. 2015).

The SVPWM technique is recurrently utilized in vector control lead and direct torque monitoring. Moreover, to 3-phase VSI while current monitoring is practiced in a revolving reference structure. The reference voltage generator is utilized in particular for vector monitoring leads. A 3-stage mathematical model is submitted herein create on a space vector impersonation (Attia 2018).

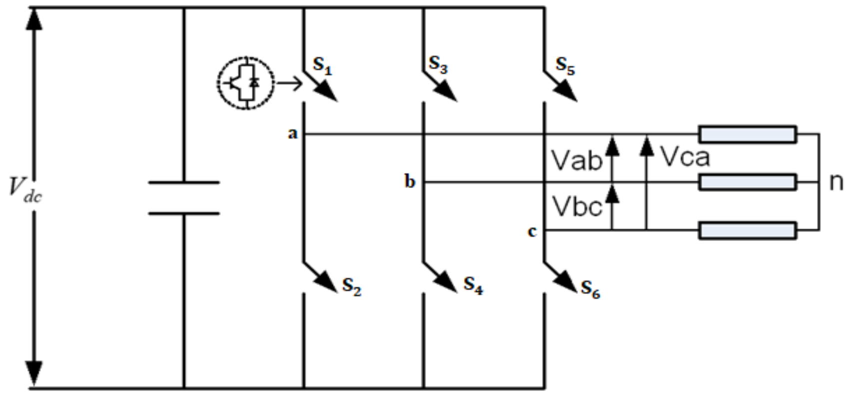

Figure 3.5 Circuit diagram voltage supply inverter

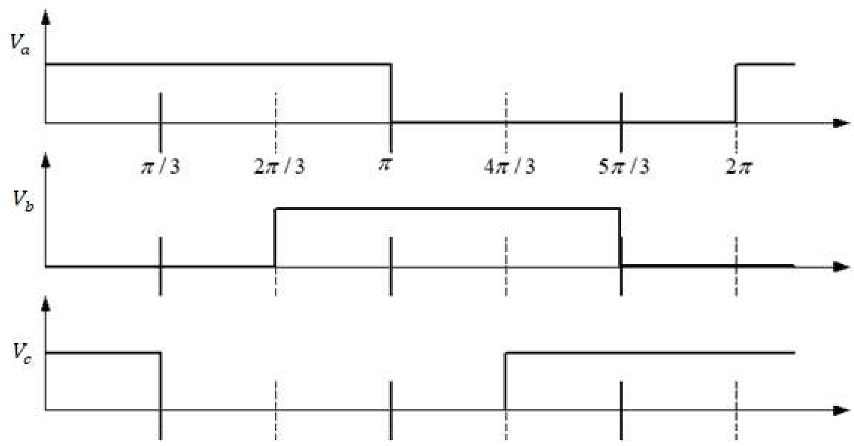

Figure 3.6 Voltage supply inverter waveform

The SVPWM impersonation of the produce voltages of the 3-phase inverter is thereafter offered. where defined is space vector as:

$$V_s = \frac{2}{3} V_{dc} \cdot (V_a + aV_b + a^2 V_c) \quad (3.11)$$

Where $a = \exp(\frac{j\,2\pi}{3})$. The space vector is a synchronous exemplification of each 3-phase quantity. It is a combination changeable and is a function of the period as opposed to phases. The phase to neutral voltages and phase to phase voltage relevance ability be expressed in the take shape of a matrix (Jambulingam 2016).

The first relation will be between phase-to-phase voltage and transition changeful vector is as follows:

$$\begin{bmatrix} V_{ab} \\ V_{bc} \\ V_{ca} \end{bmatrix} = V_{dc} \begin{bmatrix} 1 & -1 & 0 \\ 0 & 1 & -1 \\ -1 & 0 & 1 \end{bmatrix} \begin{bmatrix} a \\ b \\ c \end{bmatrix} \tag{3.12}$$

Furthermore, the connection between the transition changeful vector and the phase voltage vector is granted as follows:

$$\begin{bmatrix} V_{an} \\ V_{bn} \\ V_{cn} \end{bmatrix} = \frac{V_{dc}}{3} \begin{bmatrix} 2 & -1 & -1 \\ 0 & 2 & -1 \\ -1 & -1 & 2 \end{bmatrix} \begin{bmatrix} a \\ b \\ c \end{bmatrix} \tag{3.13}$$

From during Equation (3.13), can represents line voltages have epitomized as shown in Table 3.1.

Table 3.1 Line voltage for transition statuses (Raichurkar *et al*. 2016)

Status	Switch ON	V_{an}	V_{bn}	V_{cn}
0 & 7	2,4,6 1,3,5	0	0	0
1	1,4,6	$0.6\ V_{dc}$	$-0.3\ V_{dc}$	$-0.3\ V_{dc}$
2	1,3,6	$0.3\ V_{dc}$	$0.3\ V_{dc}$	$-0.6\ V_{dc}$
3	2,3,6	$-0.3\ V_{dc}$	$0.6\ V_{dc}$	$-0.3\ V_{dc}$
4	2,3,5	$-0.6\ V_{dc}$	$0.3\ V_{dc}$	$0.3\ V_{dc}$
5	2,4,5	$-0.3\ V_{dc}$	$-0.6\ V_{dc}$	$0.6\ V_{dc}$
6	1,4,5	$0.3\ V_{dc}$	$-0.6\ V_{dc}$	$0.3\ V_{dc}$

Moreover, conformable space vectors line voltage is roster as shown in Table 3.2.

Table 0.2 Line voltage area vectors

Status	Line voltage area vectors
0 & 7	0
1	0.6 V_{dc}
2	0.6 V_{dc} exp (j $\pi/3$)
3	0.6 V_{dc} exp (j π)
4	0.6 V_{dc} exp (j π)
5	0.6 V_{dc} exp (j $4\pi/3$)
6	0.6 V_{dc} exp (j $5\pi/3$)

As illustrated in Figure 3.5, thither of on and off patterns for the three top energy transitions for eight prospect groups. The on and off statuses of the bottom energy apparatuses are obverse to the top one and so are readily limited once the statuses of the top energy transistors are limited. As represented in Equations (3.12) and (3.13), the eight transitions vectors, line voltage (phase voltage), and Figure 3.7 shows the eight-inverter voltage vector (V0 to V7) and represent can voltage vector as shown in Table 3.3. Moreover, the output phase to phase voltages in the expression of DC-link V_{dc}.

Table 0.3 Transition states and output voltage vectors (Raichurkar et al. 2016)

Voltage	**Transition states**			**voltage line to neutr**			**Voltage phase to phase**		
	a	b	c	V_{an}	V_{bn}	V_{cn}	V_{ab}	V_{bc}	V_{ca}
V_0	0	0	0	0	0	0	0	0	0
V_1	1	0	0	0.6	-0.3	-0.3	1	0	-1
V_2	1	1	0	0.3	0.3	-0.6	0	1	-1
V_3	0	1	0	-0.3	0.6	-0.3	-1	1	0
V_4	0	1	1	0.3	0.3	0.3	-1	0	1
V_5	0	0	1	-0.3	0.3	0.6	0	-1	1
V_6	1	0	1	0.3	-0.6	0.3	1	-1	0
V_7	1	1	1	0	0	0	0	0	0

Moreover, the particular voltage must be multiplied through V_{dc} in Table 3.3.

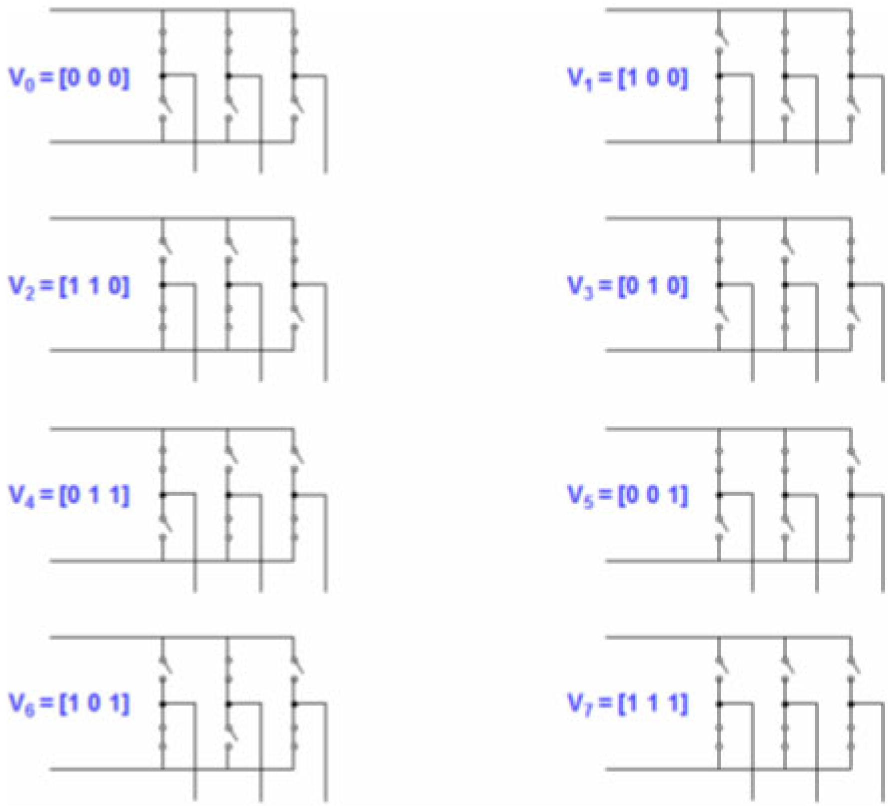

Figure 3.7 Effort vectors for the eight inverters

Additionally, PWM is frequently utilized as a lead method that is surveillance through transference and immediate torque surveillance. In a vector observation engine, this technicality is utilized to generate the indication voltage while current monitoring is applied in a revolving reference structure.

It is evident in the past part while the 3-phase VSI produces eight transition statuses including six efficient statuses and two zero statuses. Those vectors shape a hexagonal as Figure 3.8, while the ability is visible depending on six sections every extending 60 °.

The signal vector representing the 3 -phase waveform voltage is produced utilizing SVPWM during the transition between the two closest power vectors and the zero vector. To find the application period of the various vectors, which depicts the location of the change area vectors and the signal vector in the first section (Yadav 2016).

The detached line voltage place vector situations are offered in Figure 3.8.

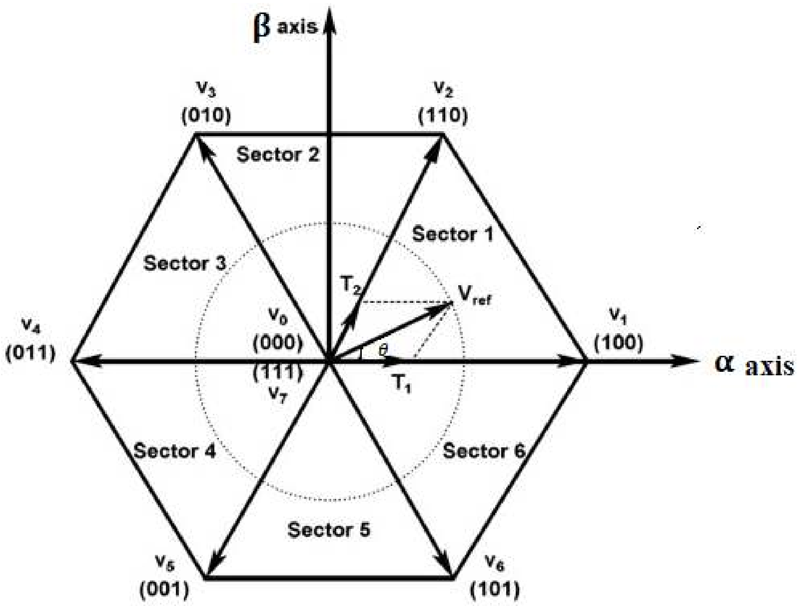

Figure 3.8 Voltage vectors and reference vector (Jambulingam 2016)

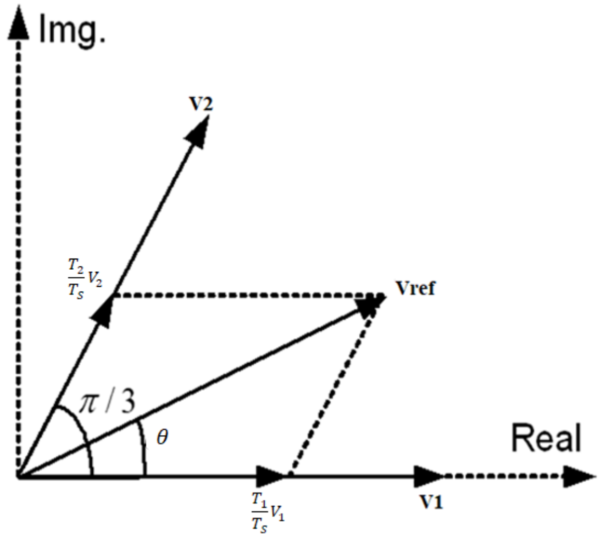

Figure 3.9 Space vector period computation (Ibrahim *et al.* 2013)

The intention of the SVPWM technicality is too convergent the V_{ref} utilizing the eight transition processes (Annapurna and Tulasiramdas 2015). One easy convergence is to make the inverter is rate output in a small T time equal to what it was in V_{ref} in the same period.

The period of application of efficient space voltage vectors from during found from Figure 3.9 as, T_1 ,$T_2$and T_0 are calculated as follows along the d axis (Jambulingam *et al.* 2016).

$$\int_0^{T_s} \bar{V}_{ref} = \int_0^{T_1} \bar{V}_1 \, dt + \int_{T_1}^{T_1+T_2} \bar{V}_2 \, dt + \int_{T_1+T_2}^{T_s} \bar{V}_0 \quad (3.14)$$

$$T_s \bar{V}_{ref} = (T_1 \bar{V}_1 + T_2 \bar{V}_2) \quad (3.15)$$

Where $0 < \alpha \leq 60$ in sector I.

$$T_1 = T_s \, (|\bar{V}_{ref}|/Vdc). \, (Sin(\frac{\pi}{3}-\alpha)/sin\frac{\pi}{3}) \quad (3.16)$$

$$T_1 = \frac{2}{\sqrt{3}} . \, Ts \, (|\bar{V}_{ref}|/Vdc). \, (Sin(\frac{\pi}{3}-\alpha) \quad (3.17)$$

Similarly,

$T_2= T_s\ (|\bar{V}_{ref}|/Vdc).\ (2/\sqrt{3}).\ \sin\alpha$ (3.18)

So, we have to compute T_1, T_2 for α varies 60°

$T_0= T_S- T_1- T_2$ (3.19)

Where $T_S = \frac{1}{f_s}$

Where T_1, T_2 and T_0 are the time interval and T_s is the switching time (switching cycle).

Each leg can adjust its state only once in the first transition cycle to achieve a set transition frequency and optimal symmetrical output from SVPWM. In half switching time, a zero-status vector is used, pursued by two neighboring efficient status vectors. The second semi of the transition time is the same as the one. The perfect transition cycle is chopped into seven sections, the zero vector is utilized for 1/4th of the perfect zero vector interval, the effective vectors are applied for semi of their implementation period, and where 1/4th of the total zero vector period on the zero vector is utilized again. At the second semi of the transition cycle, repeated is this. This is method gets harmonic SVPWM. Figure 3.10 shows the leg voltage for sector I in one switching cycle (Annapurna and Tulasiramdas 2015).

The sinusoidal prediction space vector shapes a roundish path internal to the hexagon.

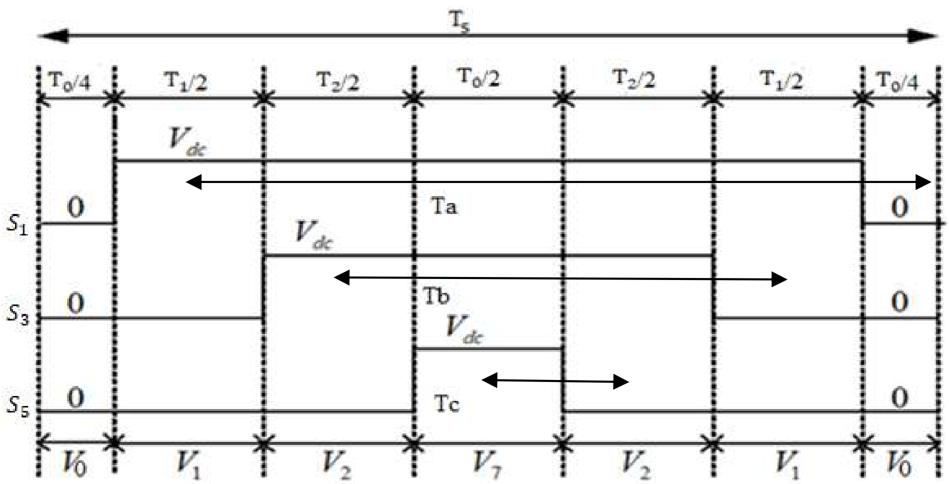

Figure 3.10 Space vector during the first sector (Jambulingam 2016)

The greatest produced voltage value that ability be realized utilizing SVPWM is the radius of the biggest ring that mastery is engraved inside the hexagon. This ring is tangent to the medium spots of the stripes connecting the terminations of the efficient space vector.

3.3 Mathematical Model of Space Vector PWM

The first step for finding the amounts of V_a , V_b ,V_c, V_{alpha} and V_{beta}, as in the equations shown below (Jambulingam 2016).

$$V_a = u(1) . sin (u(2). 2\pi. u(3)) \quad (3.20)$$

$$V_b = u(1) . \sin((u(2). 2\pi. u(3) - (\frac{2\pi}{3})) \quad (3.21)$$

$$V_c = u(1) . \sin((u(2). 2\pi . u(3)) + (\frac{2\pi}{3})) \quad (3.22)$$

$$V_{alpha} = \frac{2}{3} (V_a - 0.5 V_b - 0.5 V_c) \quad (3.23)$$

$$V_{beta} = \frac{2}{3}\left(\left(\frac{\sqrt{3}}{2}\right) V_b - \left(\frac{\sqrt{3}}{2}\right) V_c\right) \quad (3.24)$$

$$\bar{V}_{ref} = \sqrt{{V_\alpha}^2 + {V_\beta}^2} \quad (3.25)$$

$$\theta = \tan^{-1}\left(\frac{V_\beta}{V_\alpha}\right) \quad (3.26)$$

The second step is to find the suitable sector judgment, from the order that locates whose voltage range vector will be utilized to create the complex vector reference voltage $\bar{V}_{ref}$ we need to use the value V_α and V_β which on the $\alpha\ \beta$ assortment arranging to locate that section on will run on the efficient statue. Can determine which with three change values B_o,B_1 and B_2 in the following equations.

$$V_{beta} = B_o \quad (3.27)$$

Where if $V_{beta} > 1$, will be value B_o=1 , otherwise $B_o = 0$

$$\sqrt{3}V_{alpha} - V_{beta} = B_1 \quad (3.28)$$

And if $\sqrt{3}V_{alpha} - V_{beta} > 1$, thenB_1=1 ,otherwise $B_1 = 0$

$$-\sqrt{3}V_{alpha} - V_{beta} = B_2 \quad (3.29)$$

Also if $-\sqrt{3}V_{alpha} - V_{beta} > 1$, will be value B_2= 1, otherwise $B_2 = 0$

Where B_o,B_1 and B_2 are variables, and B_o, B_1 and B_2 values are determined then calculate the N value by substituting the value B_o, B_1 and B_2 in Equation (3.30).

$$N = 4\text{sign}(B_2) + 2\,\text{sign}(B_1) + \text{sign}(B_o) \quad (3.30)$$

Where sign(x) is the signed assignment. Moreover, if the sign (-) is equal to zero and if the sign (+) will be equal to (1). In shown Table 3.4 offers the connection between the number sector and the N.

Table 0.4 Connection between sector number and sector judgment

N	3	1	5	4	6	2
Sector number	1	2	3	6	5	4

The third step is the computation of the foundation voltage vector act time, from through X, Y, and Z magnitudes appear in Equations (3.31,3.32) and (3.33) (Raichurkar *et al.* 2016) To calculation of the foundation voltage vector act time and the connection between the efficient period of the basic foundation vectors T_1, T_2 and sector N , as shown in Table 3.5.

$$X= \sqrt{3}T_s \cdot (V_{beta}/V_{dc}) \quad (3.31)$$

$$Y = T_s \cdot (3\, V_{alpha} + \sqrt{3}\, V_{beta}) / (2V_{dc}) \quad (3.32)$$

$$Z = T_s \cdot (-3\, V_{alpha} + \sqrt{3}\, V_{beta}) / (2\, V_{dc}) \quad (3.33)$$

Table 0.5 The connection between effective period and voltage vector

N	1	2	3	4	5	6
T_1	-Y	X	-X	Z	Y	Z
T_2	-Z	-Y	Z	X	-X	Y

The fourth step calculates the switching operating time.

Firstly, Ta Tb and Tc ability be according to during equations below shown.

$$T_a= (T_s- T_1- T_2)/4 \quad (3.34)$$

$$T_b= -T_a + (T_1/2) \quad (3.35)$$

T_c= -$T_b + (T_2/2)$ (3.36)

The transition time is offered as the following Table 3.6, where T_{CM1},$T_{CM2}$and T_{CM3} appoints the transition of the period of the 3-phase bridge spindle energy component respectively.

Table 0.6 Represent the switching operation time

N	1	2	3	4	5	6
T_{CM1}	T_c	T_b	T_c	T_a	T_b	T_a
T_{CM2}	T_b	T_c	T_a	T_c	T_a	T_b
T_{CM3}	T_a	T_a	T_b	T_b	T_c	T_c

3.4 Voltage/Frequency Control of Induction Motor

This is the most common method for controlling an IM speed. The air gap influx volition seems to be full in this system because the applied frequency is lower when preserving the estimated source voltage. This will result in extreme stator current and flux wave distortion. As a result, the stator voltage would be reduced with the frequency to decrease a steady air-gap flow. The ratio of the stator voltage to the frequency determines the magnitude of the stator flux.

In addition, the flux remains constant if the remaining ratio is kept fixed and without change to the voltage-to-frequency. Holding the V/f constant also keeps the produced torque close to constant. This approach is more effective in terms of runtime. As a result, the constant V/f method is used to monitor the speed of the vast majority of AC speed drives. Along with the ability to monitor a wide range of speeds, This method includes a soft start feature in addition to a broad domain of velocity control (Ibrahim *et al*. 2013).

3.5 Simulation and Modelling

In this section, we worked on building and simulating SVPWM to control the velocity of a three-phase IM utilizing the V/f controller, as the motor used in this design was a squirrel cage type.

Table 3.7 represents some of the parameters that were entered into the IM during the simulation.

Table 0.7 Parameters of induction motor

Parameters	Value
Pn	3700 VA
V phase to phase	350 V
f	50 Hz
Rs	1.115 Ω
Rr	1.083 Ω
Ls	0.005974 H
Lr	0.005974 H
Lm	0.203 H
J	0.018 Kg.m^2
Friction factor	0.005752 N.m.s
Pole pairs	2
P_m	1492 kW

Figure 3.11 shows the design Matlab/Simulink sample of SVPWM based IM without using V/f control. Moreover, Figure 3.12 shows a Matlab/Simulink sample of SVPWM based IM with V/f control.

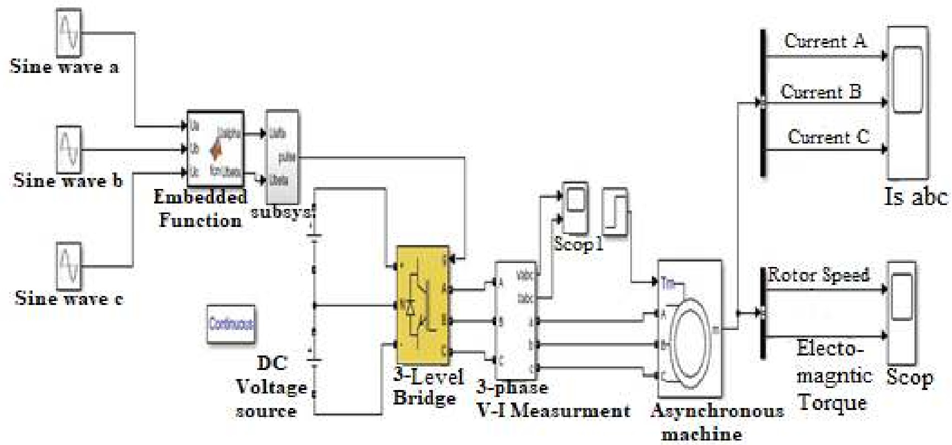

Figure 3.11 Svpwm fundamental induction motor without V/f control

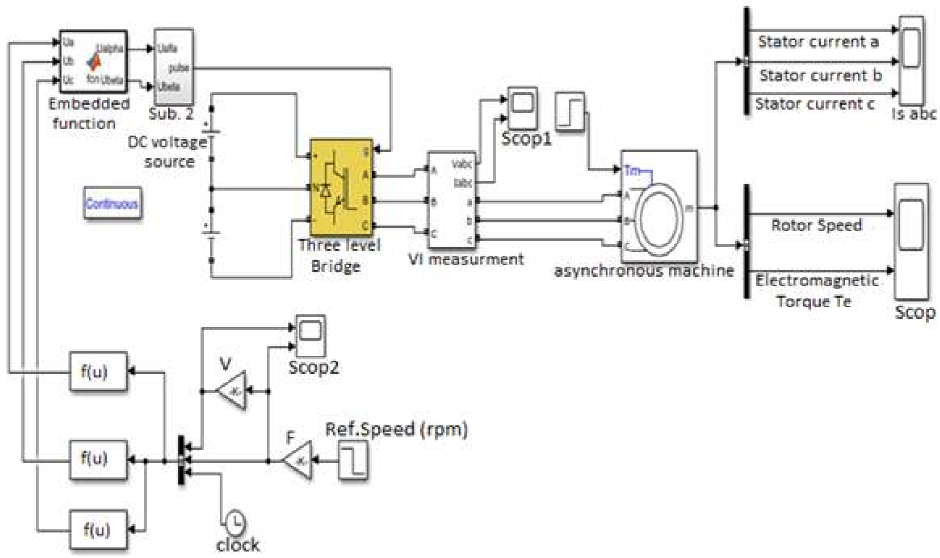

Figure 3.12 Svpwm fundamental induction motor with V/f control

Figure 3.11 represents the Matlab/Simulink model without the presence of the control unit, and Figure 3.12 represents the design of the model with the V/f control unit, the represent embedded Matlab function block in Figure 3.12 of the three-phase sine reference inputV_a , V_b and V_c as in Equations (3.20,3.21) and (3.22). Thus, it will be the same frequency in the 3-phase voltage and the angle phase shifts between phase to other phase values is 120-degree. In addition, contains this block on transformer 3-phase abc voltage to two-phase V_{alpha} and V_{beta} voltage as Equations (3.23) and (3.24), then $\alpha\beta$

voltage represents the input to subsystem II and is used to locate that sector is operated and the magnitude of the period interval for six transitions close or open.

Moreover, the subsystem (2) block represents the model of the SVPWM as shown in Figure 3.13. The step-by-step subsystem model building and creation of the SVPWM designs are shown in Figure 3.14, - Figure 3.18.

In addition, in this study, we will take the reference voltage of the supply of 350V and the applied frequency of 50 Hz to be a constant V/f ratio in the controller unit with a simulation study in two cases, in the first case we change the speed with the constant torque of the load, and the second case we change the torque of the load while the speed remains constant as depicted in the fourth division.

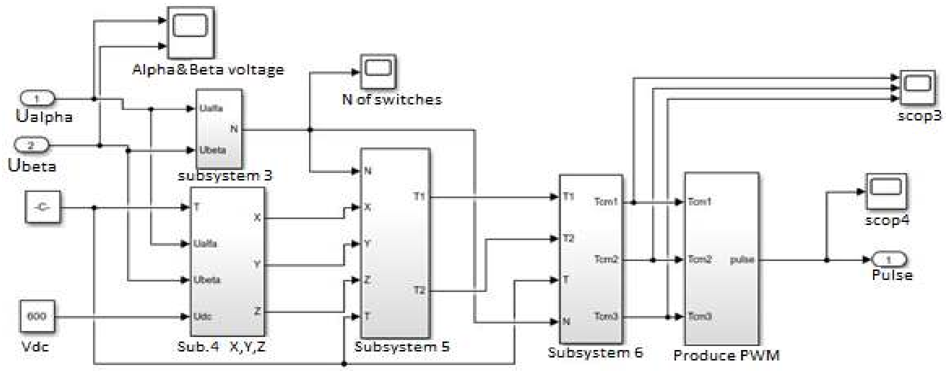

Figure 3.13 The generation of the gate pulse

Represent subsystem 3 in Figure 3.14 the value of the N block can be calculated from Equations (3.27,3.28,3.29), and (3.30), where the connection between sectors and N is offer in Table 3.3 that mastery be utilized to locate that sector is operating.

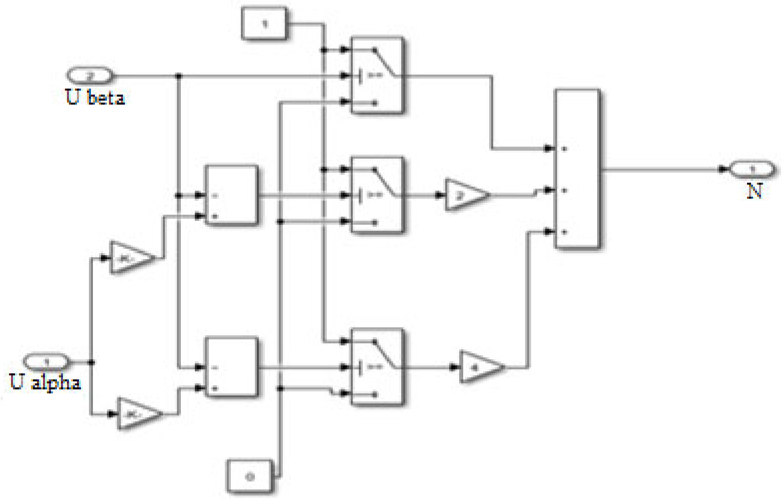

Figure 3.14 Simulation for sector judgment

Figure 3.15 and Figure 3.16 represent subsystems (4 and 5) the relationship between N and T_1, T_2 is analyzed and calculated in Equations (3.17,3.18,3.19,3.31,3.32), and (3.33) and as shown in Table 3.4. Moreover, the switching time $T_1$and T_2 has been determined and chosen foundation on the magnitude of N ($T_1$and T_2 are variable in different vectors).

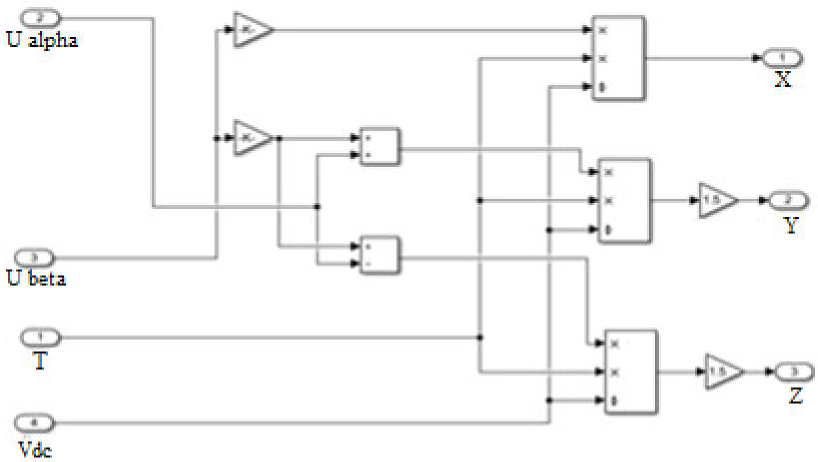

Figure 3.15 Subsystem for foundation voltage vector

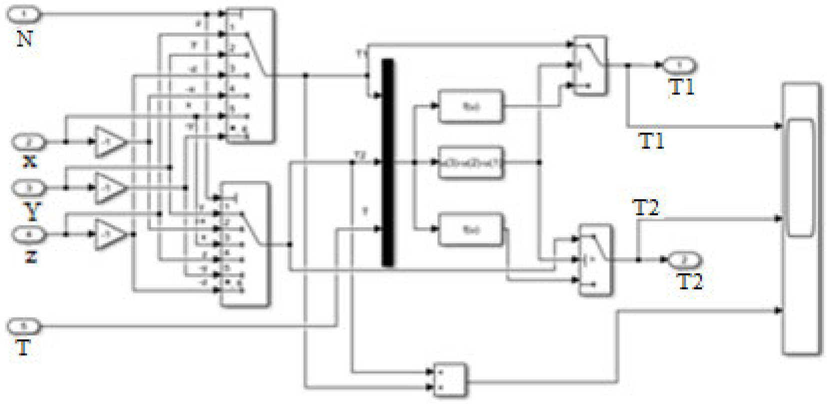

Figure 3.16 Simulation paradigm through of the effective period

Represent subsystem 6, Figure 3.17 the switching duration time Ta, Tb and Tc are calculated from during Equations (3.34,3.35), and (3.36) with the input value of T_1, T_2 and T_0 from subsystem 5, where is results as shown in Table 3.5.

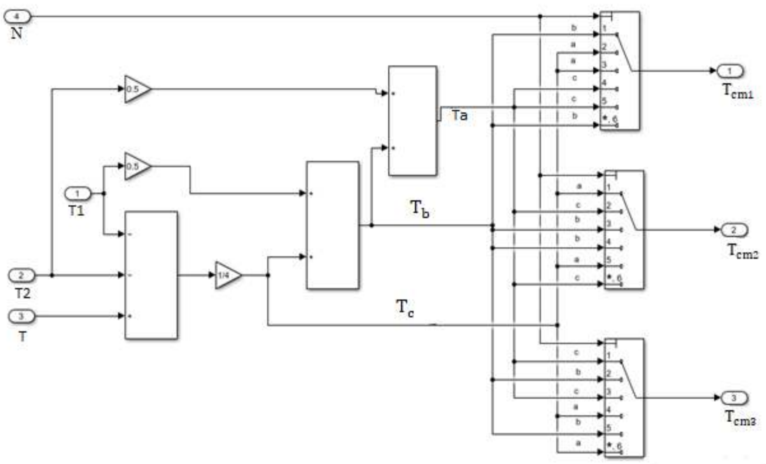

Figure 3.17 Simulation paradigm for switching operating time

Subsystem 6 is represented by Figure 3.18 which is the generation of the SVPWM pulse that will be entered into the three-level bridge block. Moreover, this block implements a three-tier bridge from forcibly selected electrical electronic devices. The remote-control circuits are series joined in parallel to every transition. In addition, the parameters used in a three-level bridge block are the number of bridge arms equal to 3, snubber resistance equal to 50 (ohm), snubber capacitance = 1e-6 (F), internal resistance Ron = 0.2 e-3 (ohm)

And IGBT / diode powered electronic device. In addition, where a three-level bridge is a source of a DC voltage supply of 600 V.

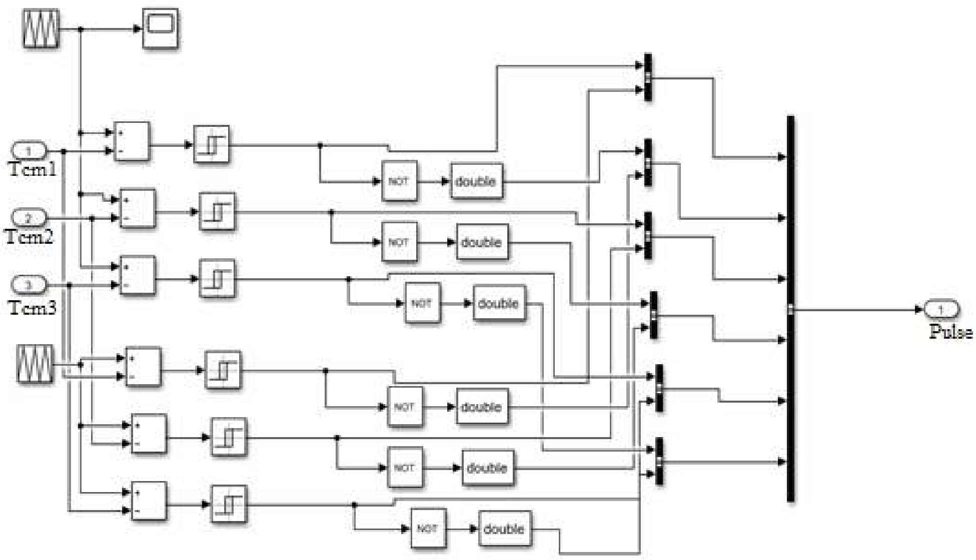

Figure 3.18 Svpwm generating model

4. RESULTS AND DISCUSSION

4.1 Results Analysis and Discussion

When performing the simulation, we obtain the following results. In Figure 4.1, the voltage output of the alpha and beta is represented after the three-phase voltage has been converted into two phases (alpha and beta).

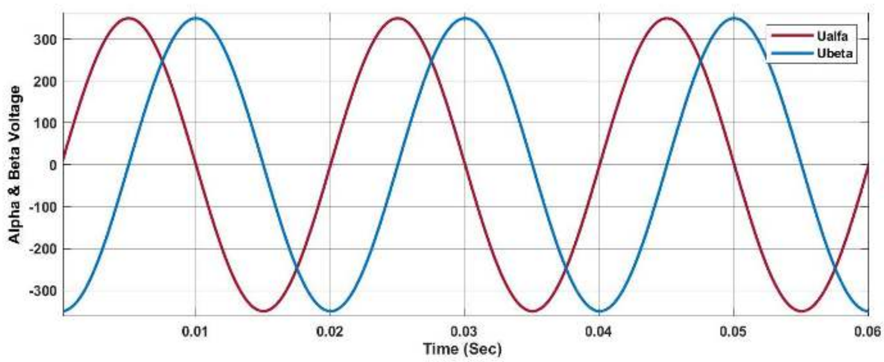

Figure 4.1 Alpha voltage and beta voltage

Figure 4.2 selector switches represents that six switches case.

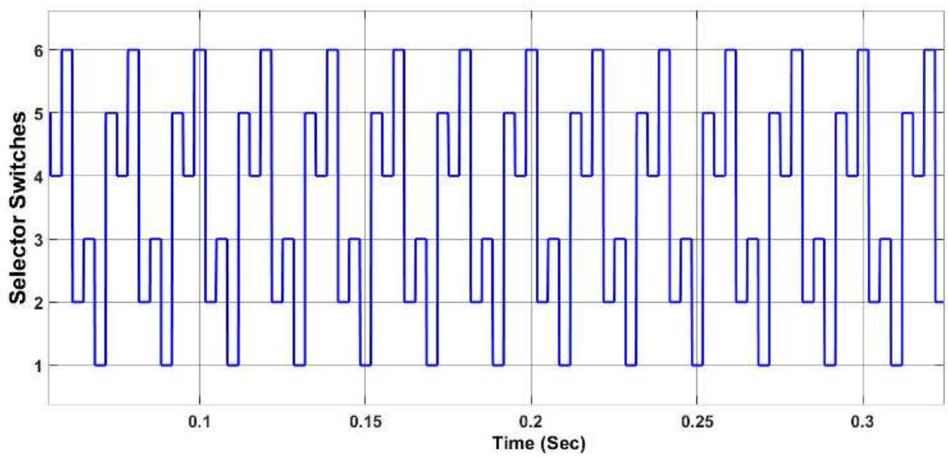

Figure 4.2 Selector switches

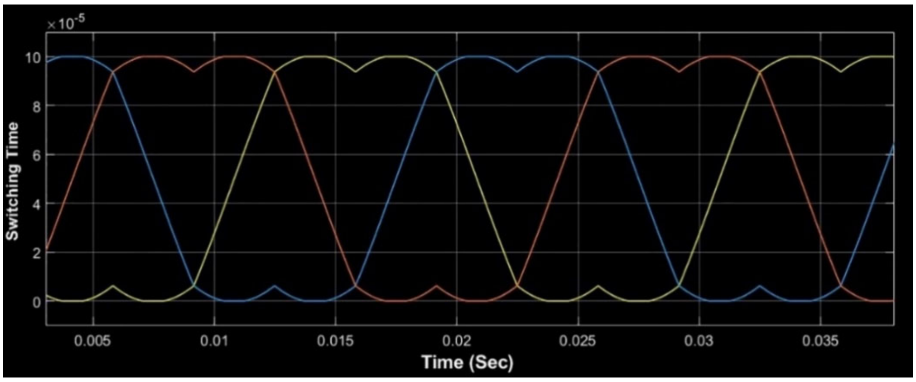

Figure 4.3 Switching operating time and the produced waveform

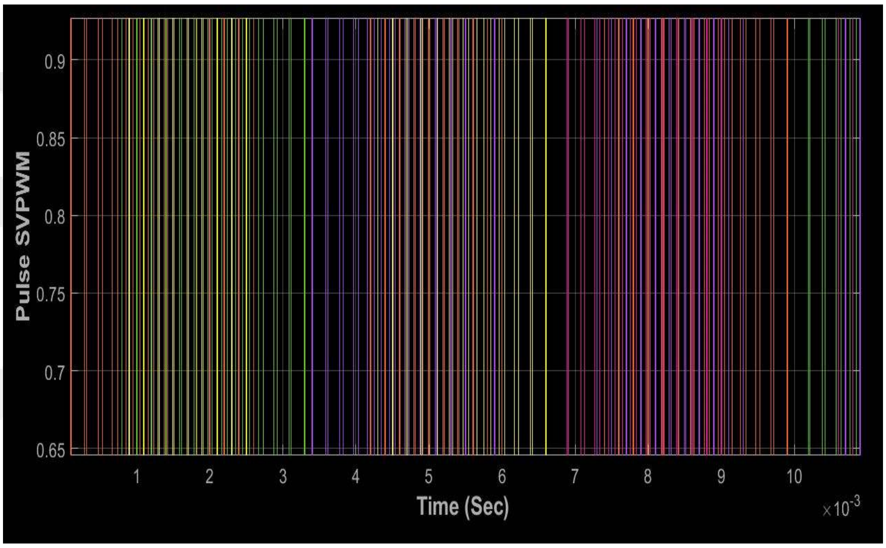

Figure 4.4 Svpwm pulse and output waveform

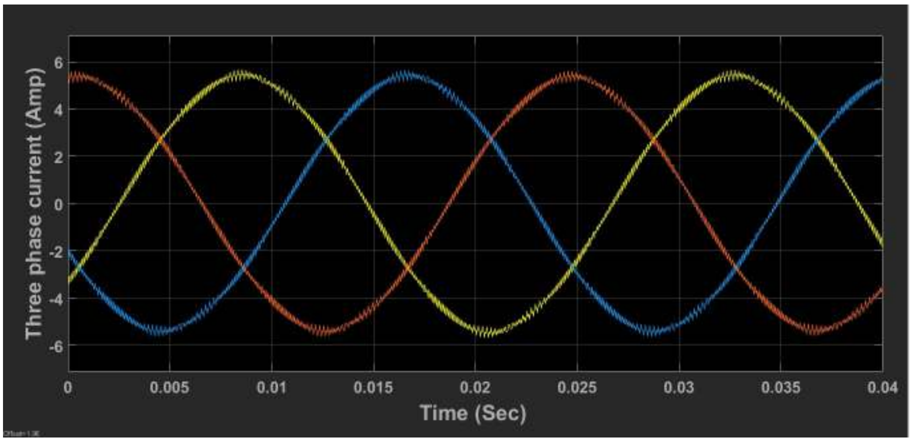

Figure 4.5 Output currents from the three-level bridge

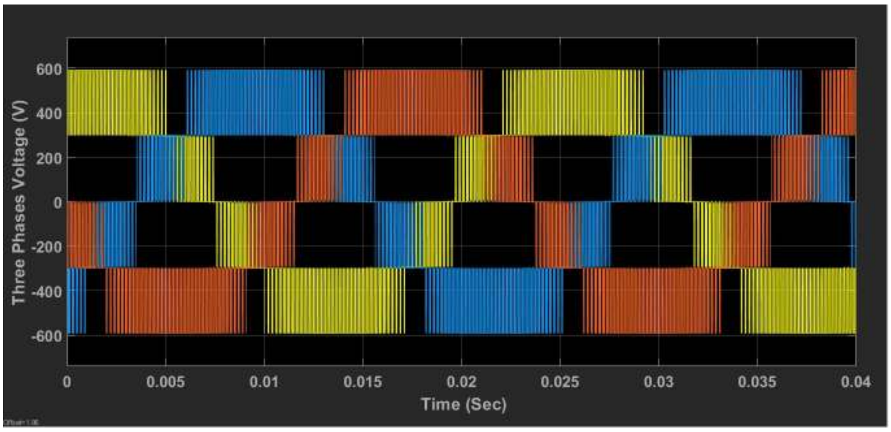

Figure 4.6 Output voltage from three-level bridge

In the first status, we will act on a variable the reference velocity, in that status, decreased the reference velocity of the induction engine from157 to 130 rps at t=1 sec. That observer on decreases the velocity of the induction engine to 1130 rps. The conformable velocity and stator currents are offered in Figure 4.7,4.8,4.9,4.10 and 4.11 respectively. Moreover, congruence to stator currents, it gets which the engine is running at stable load before and after t=1 sec.

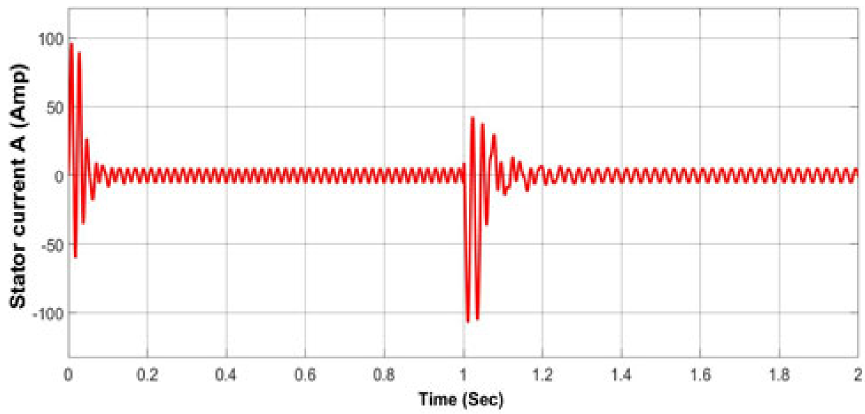

Figure 4.7 Stator current phase A

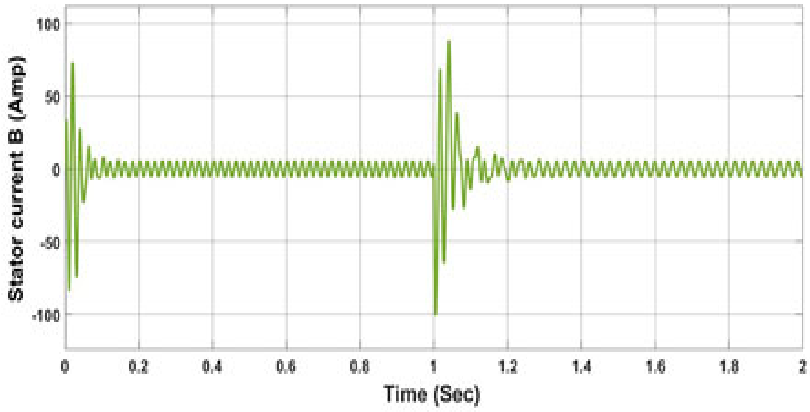

Figure 4.8 Stator current phase B

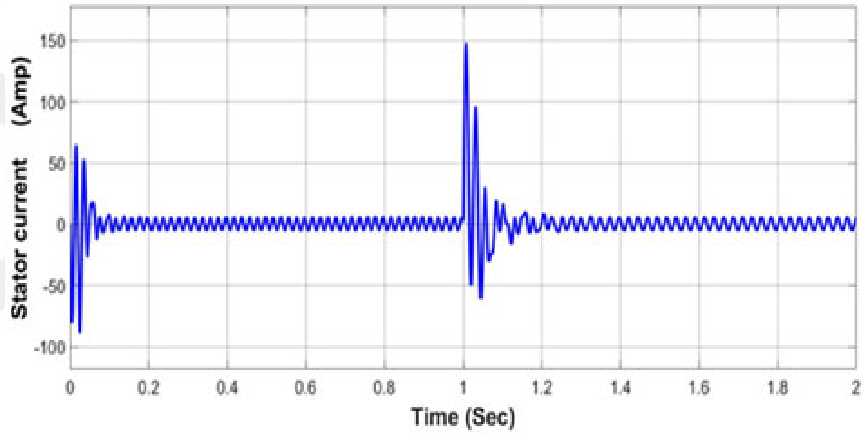

Figure 4.9 Stator current phase C

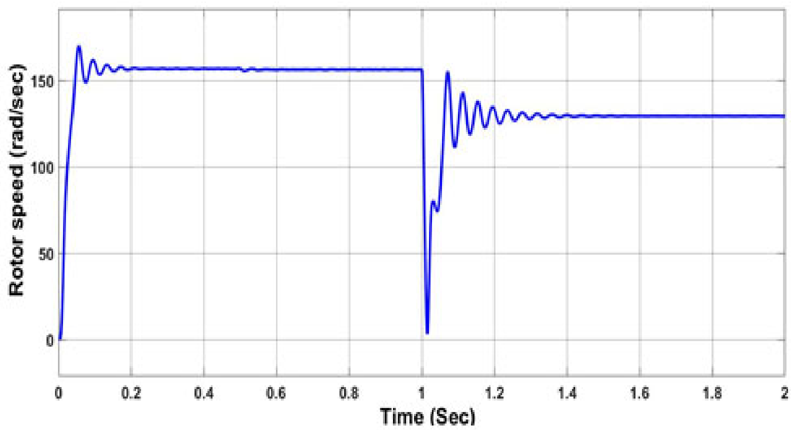

Figure 4.10 Rotor speed

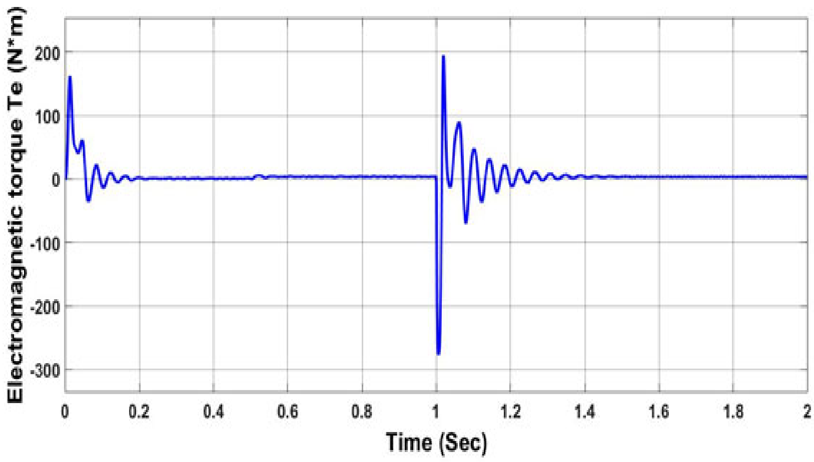

Figure 4.11 Electromagnetic torque

In the second case, we will work on changing the load torque, in that case, the load on the motor is the change from 10 N.m to 13 N.m at t = 1 sec. to put control, yonder is no variation in velocity. It obtained which the drive mastery runs at a fixed velocity during various magnitudes of torque. The conformable torque produced from the engine (electromagnetic torque), and velocity of the IM is offered in Figures 4.12 and 4.13 respectively.

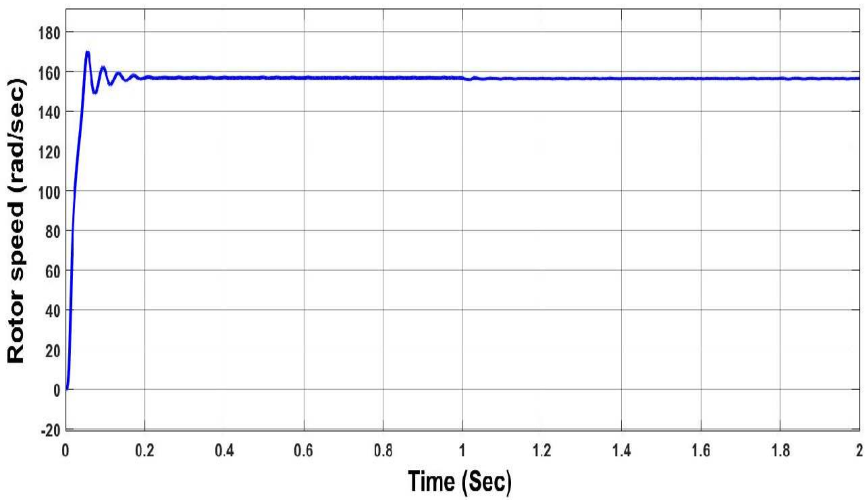

Figure 4.12 Rotor speed at reference speed constant

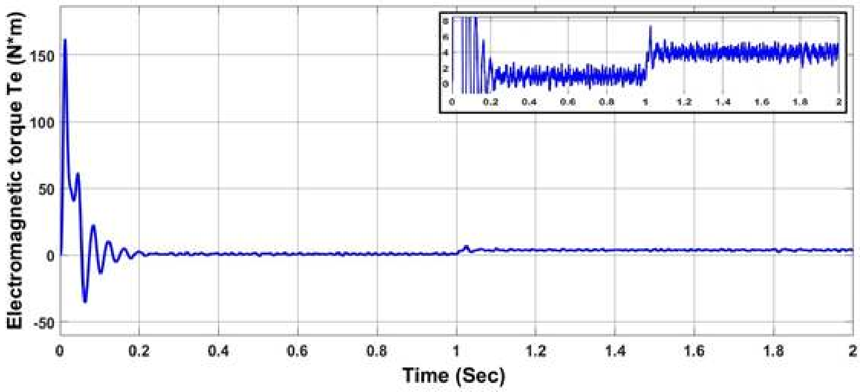

Figure 4.13 Electromagnetic torque at reference speed constant

5. CONCLUSION AND RECOMMENDATIONS

5.1 Conclusion

In that research SVPWM based on an IM for V/f controller model is designed and created during Matlab/Simulink program and also examined successfully via evaluating the parameters like stator current, torque, and speed. So that its particulars such as very stalwart, better energy factor, and high efficiency. That scheme helps to monitor the motor's speed as well as the capacity and frequency of the stator voltage. The stator effort to frequency ratio would remain fixed. Moreover, that the design and implementation of induction in Simulink are uncomplicated and trouble-free. These types of induction motors can be used in lathes, drilling machines, lifts, cranes, conveyors, industrial drives, agricultural and industrial pumps. The simulation results showed that the proposed 3-level inverter reduces ripples on torque and velocity.

5.2 Recommendation for Future Work

It is possible to work in the future to control the engine speed through the use of the following control units:

1- The speed of the IM of the PI controller.

2 - SVPWM of speed control of the IM using the fuzzy logical unit.

3- Three-phase IM uses PID technology by Arduino.

REFERENCES

Ansari, M. D. 2010. Mathematical model of asynchronous machine in matlab/simulink. International Journal of Engineering Science and Technology., 2(5):1260–1267.

Annapurna, G. and Tulasiramdas, G. 2015. Simulation and comparison of SPWM and SVPWM control for two level UPQC. Journal of Theoretical and Applied Information Technology.,78(1): 24–33.

Antonino, J. A., Climente, V., Pons, J. and Wiedenbrug, E. 2014. Advanced rotor assessment of motors operating under variable load conditions in mining facilities. IEEE Energy Conversion Congress and Exposition.,978(1): 617–621.

Aspalli, M. S., Verendra, D. and Hunagund, P. V. 2011. A new generation vlsi approach for V / f control of three-phase induction motor. International Journal of Electrical and Electronics Engineering., 1(1): 7–12.

Attia, R., Abdellah,K. and Ahmed, H. 2018. Space vector pulse width modulation for three phase cascaded H-bridge inverter. International Conference on Applied Smart Systems .,18(5): 5460–5466.

Birbir, Y. and Nogay, H. S. 2008. Design and implementation of PLC - based monitoring control system for three-phase induction motors fed by PWM inverter. IEEE Transactions on Fuzzy System., 2(3): 128–135.

Casadei, D., Serra, G. and Tani, A. 2000. Implementation of a direct torque control algorithm for induction motors based on discrete space vector modulation. IEEE Transactions on Power Electronics.,15(4): 769–777.

Da silva, E. C. and Elbuluk, M. E. 2013. Fundamentals of power electronics. In Green Energy and Technology.,59: 1442-1448.

Dinakaran, C. 2015. Modeling and simulation of speed control of induction motor by space vector modulation technique using voltage source inverter. Journal of Electrical Engineering.,15: 280–287.

Divyam, S. A., Singh, B. and Rai, J. N. 2020. Comparative analysis of PWM techniques and SVPWM operated V/f control of induction motor having different power ratings. Proceedings of the fifth International Conference on Communication and Electronics Systems., 28(1):1096–1100.

Echavarria, R., Horta, S. and Oliver, M. 1995. Three phase motor drive using IGBT's and constant V/F speed control with slip regulation. International Power Electronics Conference.,18(5): 87–91.

Emadi, A., Lee, Y. J. and Rajashekara, K. 2008. Power electronics and motor drives in electric, hybrid electric, and plug-in hybrid electric vehicles. IEEE Transactions on Industrial Electronics., 55(6): 2237–2245.

Ferdiansyah, I., Rusli, M. R., Praharsena, B., Toar, H., Ridwan and Purwanto, E. 2018. Speed control of three phase induction motor using indirect field oriented control based on real-time control system. Proceedings of Tenth International Conference on Information Technology and Electrical Engineering with Smart Technology For Better Society.,14(2):438–442.

Ferreira, F. J., Turris, E., Ge, B., Quispe, E. C. and De Almeida, A. T. 2014. Star- and delta-connected windings tolerance to voltage unbalance in induction motors. Proceedings - International Conference on Electrical Machines., ICEM ,25: 2045–2054.

Ferreira, H., Sudjoko, R. I. and Iswahyudi, P. 2019. Speed control of three phase induction motor using universal bridge and PID controller. Journal of Physics: Conference Series.,46: 1381-13887.

Husham, I. H. and Ahmed, I. J. 2015. Induction motors in stationary coordinate. Diyala Journal of Engineering Sciences.,15(2):255–265.

Hussain, A., Kubeitari, M., Alhusayn, A. and Alnahar, M. 2012. Space vector PWM simulation for three phase DC/AC inverter. International Journal of Electrical and Computer Engineering., 6(12): 1402–1407.

Hyun, J. D. and Jang, D. 2003. Space-vector PWM technique for two-phase. Journal of Engineering and Applied Sciences., 39(2): 542–549.

Ibrahim, G. E., Emad, A. and Elbesealy, M. 2013. V / F control of three phase induction motor drive with different PWM techniques. Advanced of Machnical Engineering., 14(4): 131–145.

Ibrahim Shahl, S. 2008. Three-phase induction machines IV and power electronics.IEEE Transactions on Energy Conversion.,4(1): 41–46.

Jambulingam, V. 2016. SVPWM based speed control of induction motor with three level inverter using proportional integral controller. International Journal of Electrical and Electronics Engineering., 4(1): 271–280.

Kamini, D., Shailendra, G. and Deepak, N. 2014. Speed control of 3-phase induction motor using self-tuning fuzzy PID controller and conventional PID controller. International Journal of Information and Computation Technology., 12(4):1185–1193.

Kidouche, M. and Idir, A. 2013. Direct torque control of three phase induction motor drive using fuzzy logic controllers for low torque ripple. IEEE Transactions on Fuzzy Systems, 5(2):78–83.

Kouzou, A., Mahmoudi, M. O. and Boucherit, M. S. 2009. A new 3D-SVPWM algorithm for four-leg inverters., IEEE Transactions on Smart Grid.,78(1):4244–4253.

Laithwaite, E. R. 1975. Linear electric machines and power electronics. Proceedings of the IEEE., 63(2): 250–290.

Lehuy, H. 2001. Modeling and simulation of electrical drives using matlab/simulink and power system blockset.Proceedings Industrial Electronics Conference., 15(3):1603–1611.

Majeed, M. A., Ibrahem, E. H., Mohammed, N. Q. and Habbi, M. D. 2020. Investigation of SPWM and SVPWM for induction motor drive. IOP Conference Series, Materials Science and Engineering., 45(1):745-751.

Mohamed, R., Amar, A. and Yasser, A. R. 2014. Stabilization of medium-frequency modes in isolated microgrids supplying direct online induction motor loads. IEEE Transactions on Smart Grid., 5(1):358–370.

Nagasai, K. B. and Jyothsna, T. R. 2016. Harmonic analysis and application of PWM techniques for three phase inverter. International Research Journal of Engineering and Technology., 6(3):2395–56.

Oleschuk, V. and Barrero, F. 2014. Standard and non-standard approaches for voltage synchronization of drive inverters with space-vector PWM a survey. International Review of Electrical Engineering., 9(4): 688–707.

Perales, M. A., Prats, M. M., Portillo, R., Mora, J. L., Leon, J. I. and Franquelo, L. G. 2003. Three-dimensional space vector modulation in abc coordinates for four-leg voltage source converters. IEEE Power Electronics Letters., 18(4): 104–109.

Priyanka, C. and Sobhana, O. 2016. V / F control of induction motor using space vector modulation with DC braking chopper. International Journal of Advanced Research in Electrical, Electronics and Instrumentation Engineering.,12(5):8942–8949.

Pustovetov, M. Y. 2017. A mathematical model of the three-phase induction motor in three-phase stator reference frame describing electromagnetic and electromechanical processes. Dynamics of Systems, Mechanisms and Machines, Dynamics., 5(2):1243-1249.

Riveros, J. A., Barrero, F., Levi, E., Duran, M. J., Toral, S. and Jones, M. 2013. Variable-speed five-phase induction motor drive based on predictive torque control. IEEE Transactions on Industrial Electronics., 60(8): 2957–2968.

Sandeep, S. K., Kumar, H. and Patel, A. 2014. A survey and study of different types of PWM techniques used in induction motor drive.International Journal Information Technlogy and Computer Engineering., 4(1): 18–22.

Sarkar, D. 2006. Approximate analysis of transient heat conduction in an induction motor during plugging. Proceedings of India Sixth International Conference on Power Electronics.,18(6):12–16.

Raichurkar, P. S., Seema, G. S., Shravan, K. and Jamadar, A. L.2016. V/F speed control of 3 phase induction motor using space vector modulation. International Journal of Engineering Research and Technology., 5(1):735-742.

Shafi, S. I. 2009. Three-phase induction motor construction and principle of operation and induction motor types. Journal of Physics.,12(2): 1–9.

Siemon, G. R. 1996. Electrical machines for drives and power electronics with variable frequency drives technology and applications. Journal of Intelligent and Fuzzy Systems., 13(1): 36–79.

Soni, S. K. and Gupta, A. 2013. Analysis of SVPWM based speed control of induction motor drive with using V / F control based 3 level inverter. IEEE Transactions on Industrial Electronics., 938(2):932–938.4

Sundararaju, K., Kumar, R. S. and Raj, I. G. 2017. Modeling and simulation of neural based speed controller for direct torque control of three phase induction motor. IEEE Region Tenth Annual International Conference., 1439–1444.

Swamy, R. L. and Kumar, P. S. 2008. Speed control of space vector modulated inverter driven induction motor. Lecture Notes in Engineering and Computer Science., 2169(1): 1448–1452.

Therib, M. A. 2017. Three phase induction motors introduction and parts of induction motor. Journal of Theoretical and Applied Information Technology.,36(4):2325-2331.

Umashankar, S., Shankar, V. K., Jain, G. and Kohe, M. L. 2016. Comparative evaluation of pulse width modulation techniques on effective DC link voltage utilization of grid connected inverter. International Conference on Electrical, Electronics and Optimization Techniques.,10(2): 2376–2383.

Wang, J., Ma, Y., Yang, L. and Tolbert, L. M. 2013. Power converter-based three-phase induction motor load emulator. Conference Proceedings - IEEE Applied Power Electronics Conference and Exposition.,14(3): 3270–3274.

Wong, Y. K., Chan, T. F. and Shi, K. L. 1997. Modeling of the three-phase induction motor using simulink. IEEE International Electric Machines and Drives Conference Record.,5(1): 6–8.

Yadav, S. 2016. Analysis of speed control of three phase induction motor by V / f method using SVPWM technique. IEEE Transactions on Industrial Electronics., 2(3): 18–23.

Yaseen, F. R. and Nasser, W. H. 2018. Design of speed controller for three phase induction motor using fuzzy logic approach. Iraqi Journal of Computer, Communication, Control and System Engineering., 18(3): 12–25.

Yanxin, L., Qinfen , L., Yunyue, Y. and Zhu, Z. Q. 2013. Investigation of forces in linear induction motor under different slip frequency for low-speed maglev application. IEEE Transactions on Energy Conversion., 28(1):145–153.

Zenginobuz, G., Cadirci, I., Ermish, M. and Barlak, C. 2001. Soft starting of large induction motors at constant current with minimized starting torque pulsations. IEEE Transactions on Industry Applications., 37(5): 1334–1347.

Zhou, J. H., Chen, C., Zhang, X. W. and Chen, Y. A. 2013. Reducing voltage energy-saving control method of induction motor. International Conference on Electrical Machines and Systems., 26(3):2159–2162.

Zimmer, O. 2000. A method of magnetic storage of ultra-cold neutrons for a precise measurement of the neutron lifetime. Journal of Physics Nuclear and Particle Physics., 14(1): 67–77.

CURRICULUM VITAE

Name and Surname : Ahmed Harb NAJD

Education

MSc	Çankırı Karatekin University Graduate School of Natural and Applied Sciences Department of Electrical and Electronics Engineering	2020-Present
Undergraduate	Basra University Faculty of Engineering Department of Electrical Engineering	1996-2001

Work Experience

Year	**Institution**	**Position**
2008-Present	Ministry of Oil Department of Electrical Engineering	Iraq-Baghdad

Academic Activities

1. Najd, A. H., Korkmaz, F., and Hammood, H. F. 2021. SVPWM based speed control of induction motor with three level inverter using V/f controller. Advances in Mechanics, 9(3): 1329-1348.